Title:

Dual-specific autophosphorylation of kinase IKK2 enables phosphorylation of substrate IκBα through a phosphoenzyme intermediate

Prateeka Borar[1], Tapan Biswas[2,#], Ankur Chaudhuri[3,#], Pallavi Rao T[4], Swasti Raychaudhuri[4], Tom Huxford[5], Saikat Chakrabarti[3] Gourisankar Ghosh[2] & Smarajit Polley[1,*]

[1]Department of Biological Sciences, Bose Institute, Kolkata, India; [2]Department of Chemistry and Biochemistry, University of California San Diego, La Jolla, USA; [3]Structural Biology and Bioinformatics Division, CSIR-Indian Institute of Chemical Biology, Kolkata, India; CSIR-[4]Centre for Cellular and Molecular Biology, Uppal Road, Hyderabad 500007, India; [5]Department of Chemistry and Biochemistry, San Diego State University, San Diego, USA.

[#] These two authors have contributed equally to this work.

*Correspondence to be addressed to: spolley@jcbose.ac.in, smarajit.polley@gmail.com

Abstract:

Rapid and high-fidelity phosphorylation of two serines (S32 and S36) of IκBα by a prototype Ser/Thr kinase IKK2 is critical for fruitful canonical NF-κB activation. Here, we report that IKK2 is a dual specificity Ser/Thr kinase that autophosphorylates itself at tyrosine residues in addition to its activation loop serines. Mutation of one such tyrosine, Y169, located in proximity to the active site, to phenylalanine, renders IKK2 inactive for phosphorylation of S32 of IκBα. Surprisingly, auto-phosphorylated IKK2 relayed phosphate group(s) to IκBα without ATP when ADP is present. We also observed that mutation of K44, an ATP-binding lysine conserved in all protein kinases, to methionine renders IKK2 inactive towards specific phosphorylation of S32 or S36 of IκBα, but not non-specific substrates. These observations highlight an unusual evolution of IKK2, in which autophosphorylation of tyrosine(s) in the activation loop and the invariant ATP-binding K44 residue define its signal-responsive substrate specificity ensuring the fidelity of NF-κB activation.

Introduction:

Protein kinases bestow novel identity to their substrates by adding phosphate moieties at the site of modification that often play key regulatory roles in a diverse array of signaling events. For example, inflammatory or pathogenic signals trigger precisely regulated induction of the transcription factor NF-κB in metazoans(Hoffmann and Baltimore, 2006) that depends upon the upstream activation of the Inhibitor of κB Kinase-complex (IKK-complex), comprising two catalytic subunits, IKK1 (also known as IKKα) and IKK2 (or IKKβ), and an essential regulatory scaffolding protein, NEMO (IKKγ)(DiDonato et al., 1997; Rothwarf et al., 1998; Zandi et al., 1997). IKK2 activity is maintained at a very low basal level in resting cells(Ghosh and Karin, 2002; Hacker and Karin, 2006; Hinz and Scheidereit, 2014; Liu et al., 2012). Upon activation, IKK2 phosphorylates the N-terminus of IκBα (Inhibitor of κBα) protein specifically at two Serine residues (S32 and S36) marking it for ubiquitinylation-mediated proteasomal degradation (Figure 1A). Signal-responsive phosphorylation of IκBα refers to the phosphorylation of S32 and S36 by the IKK-activity. Degradation of IκBα liberates NF-κB to

execute its gene expression program (Hayden and Ghosh, 2008; Hinz and Scheidereit, 2014; Karin and Ben-Neriah, 2000; Scheidereit, 2006). Mutation of both S32 and S36 to alanine residues converts IκBα into a non-phosphorylatable super-repressor of NF-κB(Brown et al., 1995; Lin et al., 1995). Furthermore, IKK possesses exquisite specificity for these two serines, and it fails to phosphorylate IκBα when S32 and S36 are mutated even to another phosphorylatable residue, threonine(DiDonato et al., 1997).

IKK2 is an essential Ser/Thr kinase that ensures the activation of a particular signaling cascade - NF-κB, with high fidelity despite its reported pleiotropy in other contexts(Antonia et al., 2021; Schröfelbauer et al., 2012; Schrofelbauer and Hoffmann, 2011). IKK2 is a multidomain protein consisting of a kinase domain (KD) followed by a Ubiquitin-like domain (ULD) and the scaffold dimerization domain (SDD) (Figure 1B). IKK2 toggles between inactive and active states based on the phosphorylation status of two serine residues (S177 and S181; S176 and S180 in the case of IKK1) within its activation loop (activation loop) in the KD(Huse and Kuriyan, 2002; Liu et al., 2013; Polley et al., 2013; Xu et al., 2011). Replacement of these two serines with phospho-mimetic glutamate residues (S177E, S181E; henceforth EE) renders the kinase constitutively active. IKK2 is reported to be primed through phosphorylation at S177 by the upstream kinase TAK1 that leads to auto-phosphorylation at S181, thus rendering the kinase fully active in cells(Zhang et al., 2014). However, oligomerization upon association with NEMO, in the presence of linear or Lys-63 linked poly-ubiquitin (Ub) chains or at a high concentration of IKK2, also enables *trans* auto-phosphorylation at S177 and S181(Chen, 2012; Du et al., 2022; Ea et al., 2006; Polley et al., 2013). It was also shown that NEMO not only helps in the activation of the IKK-complex, but also ensures that the IKK-activity is well directed towards IκBα in the inhibitor bound transcriptionally inactive NF-κB (NF-κB: IκBα complex)(Schröfelbauer et al., 2012). Activated IKK2 phosphorylates IκBα specifically at residues S32/S36, for which the C-terminal SDD of IKK2 (residue range 645-756) is critical – a shorter construct of IKK2 lacking the NBD and SDD displayed CK2-like activity that did not retain the exquisite specificity of IKK2 to phosphorylate the S32/36 of IκBα

(Shaul et al., 2008). Other sites of IκBα e.g., the residues in the C-terminal PEST region that contains proline (P), glutamic acid (E), serine (S) and threonine (T) residues, but not S32/S36, can be phosphorylated by various kinases(Barroga et al., 1995; Tergaonkar et al., 2003). The role of IκBα-phosphorylation at sites other than the signal responsive S32/S36 phosphorylation in NF-κB activation and signaling is elusive. These findings underscore the ability of IKK2 to function specifically in order to guarantee rapid NF-κB activation in canonical signaling. It is however, still not fully understood how IKK2 achieves its exquisite specificity towards S32/S36 of IκBα to mark it for proteasomal degradation that liberates active NF-κB dimers.

Here we report an in-depth analysis of the catalytic features of IKK2 that revealed that IKK2 undergoes multisite autophosphorylation and can phosphorylate its own tyrosine residue(s) in addition to its own serines or the serines of its substrate IκBα, i.e., IKK2 possesses dual specificity. This phosphorylation at tyrosine residue(s) is autocatalytic. This phosphorylation at tyrosine residues is dependent upon the prior activation of IKK2 via activation loop S177/S181 phosphorylation, and is critical to phosphorylation of signal responsive S32/S36 of IκBα. Mutation of Y169 of IKK2 to phospho-ablative phenylalanine severely compromised phosphorylation of IκBα at S32. Mutation of Y188 to phenylalanine rendered the kinase practically inactive *in vitro*. IKK2 activity towards signal responsive S32/S36 of IκBα was severely compromised in MEF cells reconstituted with these two mutant IKK2s in response to treatment with TNFα. We also observed that mutation of the conserved ATP-interacting residue K44 in IKK2 to methionine leads to a loss of tyrosine as well as S177,S181 auto-phosphorylation activity of the kinase along with its ability to phosphorylate S32/S36 of IκBα, thereby clearly suggesting a critical role of this Lysine residue in regulating IKK2's kinase activity for tyrosine as well as serine phosphorylations. Interestingly, IKK2 K44M retained non-specific kinase activity referring to phosphorylation of IκBα at residues other than S32 and S36. Furthermore, we observed that, after auto-phosphorylation at tyrosine, IKK2 can phosphorylate IκBα in the absence of exogenous supply of ATP, as long as ADP is

present in the reaction. Overall, our results reveal unique, and likely transient, autophosphorylated intermediates of IKK2 that appear to be critical in relaying phosphoryl group(s) specifically to S32/S36 of IκBα rather than following the conventional mode of phosphate group transfer directly from ATP to the substrate seen in eukaryotic protein kinases. IKK2 thus ensures fidelity of NF-κB activation. Recent reports in other kinases indicate that multisite (auto)phosphorylation is a major determinant in regulating function of respective kinases and regulation exerted by those kinases. Our study adds another layer of regulation and critical nature of such autophosphorylation that plays a significant biological role in metazoans.

Results:

IKK2 undergoes auto-phosphorylation at uncharacterized sites:

Signal-induced phosphorylation of activation loop Ser177/Ser181 marks the general activation of IKK2 (Figure 1B). Hyperphosphorylation of several other serines located within the flexible C-terminal region of IKK2, spanning amino acid 701 to the end (Figure 1B), has been reported to down-regulate IKK2 activity in cells (Delhase et al., 1999). Furthermore, ectopically overexpressed IKK2 was found to be capable of autophosphorylating these two serines in the activation loop in *trans* even in the absence of an activating physiological signal {Polley, 2013 #27}. Indeed, recombinantly purified FL IKK2WT is capable of autophosphorylation *in vitro* when incubated with γ^{32}P-ATP that increases with the time of incubation (Figure 1C), possibly at multiple sites as indicated by the spread-out of slower migrating phospho-IKK2 band. We also observed that autophosphorylation of IKK2 occurred irrespective of the presence of its cognate binding partner NEMO and *bonafide* substrate IκBα (Figure 1D). An *in vitro* kinase assay using a kinase inactivating mutant, IKK2 K44M along with the WT kinase using γ^{32}P-ATP as the phosphor-donor confirmed that the above-mentioned phosphorylation of IKK2 was indeed autophosphorylation and not due to an unrelated kinase copurified with IKK2 as IKK2 K44M lacked both IκBα (substrate) and autophosphorylation activities (Figure S1A). Lys44 is the ATP-binding invariant lysine residue

in IKK2 that is conserved in STYKs, mutation to which to Met is expected to greatly reduce or eliminate the kinase activity. These observations were further supported by another *in vitro* radioactive kinase assay performed in the presence or absence of an IKK-specific ATP-competitive inhibitor, Calbiochem Inhibitor VII (Figure 1E), that inhibits specific phosphorylation of S32/36 on IκBα (Figure S1B). In both cases kinase and kinase-substrate reactions were incubated for 30 minutes with the inhibitor prior to adding the phosphor-donor, γ^{32}P-ATP or cold ATP. Purification status of recombinant FL IKK2 WT and FL IKK2 K44M proteins used in this study are shown in Figure S1C, along with LC MS/MS study performed on the FL IKK2 K44M (Figure S1D).

Next, we used different versions of the IKK2 protein where all previously known phosphorylation sites were lacking: Ser177 and 181 were mutated to phosphor-mimetic Glu (EE; this version of IKK2 is known to be constitutively active (Zandi et al., 1998)), and the C-terminal serine-rich region was truncated to different extents. The shortest construct, Δ664EE that entirely lacked the flexible C-terminus (670-756) was further subjected to limited proteolysis using trypsin to eliminate residues, if any, from the flexible ends of the enzymes and this trypsin-treated IKK2 was purified prior to *in vitro* kinase assays. Each of these constructs was active in phosphorylating itself and the substrate IκBα (Figure 1F). The occurrence of autophosphorylation despite the absence of activation loop serines and serines within the C-terminus strongly suggested the presence of hitherto uncharacterized sites of autophosphorylation in IKK2.

Auto-phosphorylation of IKK2 reveals its dual specificity:

IKK2 is known as a *bonafide* Ser/Thr kinase that undergoes autophosphorylation. In the previous section, we found that IKK2's autophosphorylation activity might extend beyond the previously characterized site(s). We asked if it is a dual specificity kinase. To this end, we unexpectedly observed *de novo* auto-phosphorylation of IKK2 on tyrosine residues (Figure 2A, middle panel) along with the anticipated auto-phosphorylation of activation loop serines (Figure 2A, upper panel) when IKK2 was incubated with Mg^{2+}-ATP for various time periods.

Increase in autophosphorylation of activation loop-S177/181 with time indicates inhomogeneous and incomplete phosphorylation of activation loop-S177/181 in the recombinant IKK2 when purified from Sf9 cells. To circumvent the specificity-bias of the pan-phosphotyrosine antibody used in Figure 2A, we used another phospho-tyrosine specific antibody, which confirmed that detection of *de novo* phosphotyrosine on IKK2 was independent of the source of the antibody used (Figure 2B). The tyrosine auto-phosphorylation was abolished in the presence of an IKK-specific inhibitor, Inhibitor VII (Figure 2C), and the IKK2-K44M mutant (kinase inactivating) did not display any tyrosine autophosphorylation when incubated with ATP unlike WT IKK2 (Figure 2D). IKK2 autophosphorylation assay performed in presence of different concentration of Urea revealed that its tyrosine-autophosphorylation was abolished at urea concentration beyond 1M (Figure S2A). A more sensitive assay with γ^{32}P-ATP as the phospho-donor also indicated that urea concentrations above 1M abolished both pan-auto-phosphorylation and substrate (IκBα) phosphorylation of IKK2 (Figure S2B). These results confirmed that IKK2 is a dual specificity kinase that not only phosphorylates Ser on substrates, but also phosphorylates its own Ser and Tyr residues. The fact that activities of IKK2 towards S32 and S36 of IκBα and its own tyrosine residue(s) were affected similarly by various kinase inhibitors, both general (AMPPNP and Staurosporine) and IKK-specific (MLN-120B, TPCA, Inhibitor VII) (Figure S2C), confirm that both substrate phosphorylation and autophosphorylation activities of IKK2 are carried out by the same active site. We further observed that the C-terminal NEMO binding domain (NBD) was not required for autocatalytic dual specificity of IKK2 as various truncated versions of IKK2 (lacking NBD) were capable of phosphorylating itself on tyrosine residue(s), and phosphorylating IκBα at signal-responsive S32 and S36 (Figure 2E). Assessment of phospho-Ser and Tyr on a constitutively active NBD-deficient IKK2 (IKK2$^{\Delta 664}$EE) monitored by monoclonal phospho-serine and phospho-tyrosine antibodies revealed *de novo* tyrosine autophosphorylation of the kinase while *de novo* serine autophosphorylation (if any) was not discernible in this assay condition (Figure 2F). The phospho-ablative S177A, S181A (AA; non-

phosphorylatable activation loop) mutant of IKK2 that was incapable of phosphorylating S32/36 of IκBα (Figure S2D), also lacked tyrosine autophosphorylation activity (Figure 2G) in *in vitro* kinase assay suggesting that activation loop S177/S181 serine phosphorylation is essential in conducting dual specificity of IKK2.

Dual-specific autophosphorylation is critical for IKK2's function

Previous reports suggested that phosphorylation of IKK2 on Y169, Y188 and/or Y199 was critical for its function(Darwech et al., 2010; Meyer et al., 2013). Our mass spectrometric analyses identified multiple tyrosine residues to be phosphorylated, e.g., Y169, Y188, Y325 (Figure S3A). To glean into the structural plausibility of tyrosine phosphorylation within the activation loop, we compared available structural models of human IKK2 (PDB ID: 4KIK, 4E3C) (Liu et al., 2013; Polley et al., 2013). In the active state conformers, the position and conformation of Tyr169 appears to be well-poised for accepting a phosphate from ATP (Figure S3B) intramolecularly. A superposition of IKK2 with a pseudo-substrate-bound PKA shows that the hydroxyl of Tyr169 in IKK2 projects toward the γ-phosphate of ATP similarly to the serine hydroxyl on the PKA inhibitor pseudo-substrate(Knighton et al., 1991; Nolen et al., 2004) (Figure S3B & C). Interestingly, Y169 is the DFG+1 (DLG in case of IKK2 and IKK1) residue while Y188 (equivalent to Y204 of PKA) is located at the end of activation loop prior to the conserved APE motif (Figure 3A & B). It was previously established that the DFG+1 position is crucial for defining the substrate specificity of a kinase(Chen et al., 2014). Y188 counterpart Y204 of PKA is reported to allosterically modulate PKA activity by altering its conformational entropy(Ahuja et al., 2017; Yang et al., 2005). In order to understand the functional consequence of dual-specific autophosphorylation of IKK2, we further focused our attention to Y169 and Y188 as they are located in the activation loop of the kinase along with the previously described K44M mutant.

Firstly, we wanted to check the effect of autophosphorylation on IKK2 activity by using the kinase inactivating K44M mutant that was found to be incapable of tyrosine autophosphorylation (Figure 2D) and fails to undergo autophosphorylation of the activation

loop serines (Figure S3D). Interestingly, IKK2-K44M showed a very weak auto-phosphorylation activity compared to WT IKK2 but phosphorylated full-length WT IκBα robustly albeit much less efficiently than WT IKK2 in a radioactive *in vitro* kinase assay (Figure 3C). However, IKK2-K44M was unable to specifically phosphorylate S32/S36 of IκBα (Figure 3D). These seemingly contrasting results possibly reflects phosphorylation of the PEST region of FL IκBα in the radioactive kinase assays as they report pan-phosphorylation of a substrate (Figure 3C & D). In addition, IKK2-K44M phosphorylated FL IκBαAA more efficiently than FL IκBα WT unlike WT IKK2 that phosphorylated FL IκBα WT much more efficiently than FL IκBαAA (Figure S3E). It indicates that IKK2-K44M retained non-specific kinase activity to some extent while lost functionally relevant specificity towards the S32, S36 of IκBα. We subjected 20ug of FL IKK2 K44M protein used in the above studies to LC-MS/MS analysis, which did not detect any significant contaminating kinase from Sf9 cells. It is noteworthy that an equivalent K to M mutation in Erk2 also did not abolish the basal activity, but rather retained ~5 % of it(Robbins et al., 1993).

Next, we wanted to understand the functional relevance of tyrosine autophosphorylation using two tyrosine-phosphoablative mutants of IKK2 (FL IKK2-Y188F and FL IKK2-Y169F), both of which showed severe reduction in activity in an *in vitro* kinase assay (Figure 3E). Since the DFG+1 residue in kinases (Y169 in IKK2) is known to dictate its specificity, we created different single mutants of IκBα where S32 and S36 were independently altered to either alanine (phosphoablative) or glutamic acid (phosphomimetic) residues. FL IKK2-Y169F displayed drastically reduced level of kinase activity towards S36A/E mutants of IκBα while that for the S32A/E mutants were minimally affected compared to the WT substrate (Figure 3F). Reduction of phosphorylation S36A/E by the WT IKK2 was less severe compared to that by the Y169F mutant kinase (Figure S3F). The above observations suggest that the presence of Tyr (and possibly its phosphorylation) is critically important for signal-responsive phosphorylation of IκBα.

Next, we reconstituted IKK2 knock-out mouse embryonic fibroblast (*ikk2*$^{-/-}$ MEF) cells with WT, Y169F and Y188F mutants of IKK2, and measured signal-induced activation of IKK2 upon TNF-α treatment. IKK2 activity is significantly reduced in Y169F and nearly abolished in Y188F (Figure 3G**)**. Phosphorylation of activation loop serines of the less active Y169F mutant, nonetheless, was only marginally defective (Figure S3G) suggesting that activation loop phosphorylation is necessary but not sufficient for IKK2 to become fully active. Together, these results hint at an unreported communication between the phosphorylation of Y169 of IKK2 and that of S32 of IκBα.

Structural analyses of IKK2 autophosphorylation:

To get a more comprehensive picture, it is necessary to analyze at least three phosphorylated states of IKK2: unphosphorylated (UnP-IKK2), phosphorylated at S177 and S181 (p-IKK2), and phosphorylated at Y169, S177 and S181 (P-IKK2). We took advantage of computational approaches using molecular dynamic (MD) simulations and flexible molecular docking (see methods). MD simulation was performed for 200ns for each of these three states of IKK2, unphosphorylated and phosphorylated. Phosphorylation at S177, S181 increased the stability of the kinase, which was further increased by the phosphorylation at Y169 as evidenced by a gradual decrease in the total energy of system (Figure 4A). A striking enhancement in stability of IKK2 upon this auto-phosphorylation is reflected in the change of Tm from ~ 40 °C to ~ 50 °C in differential scanning calorimetry (DSC) scans in the presence of ADP and ATP (Figure S4A). This behavior supports our observation in MD simulation, and tallies with increased solubility of IKK2 observed after auto-phosphorylation that was essential for its successful crystallization (Polley et al., 2013).

Interestingly, RMSD values increased with more phosphorylation (Figure 4B) despite phosphorylation-induced stabilization, P-IKK2 showed the highest RMSD followed by p-IKK2 and UnP-IKK2, indicating increased internal motion in the kinase as a result of phosphorylation. It may be noted that, the changes in total energy and RMSD are consistent throughout the course of simulation though the magnitude is small. We found that,

phosphorylation at S177, S181 and S177, S181, Y169 induced distinct structural alteration in the KD when compared with the unphosphorylated version (Figure 4C, models shown separately in Figure S4B). Careful analyses of the trajectory of RMSF values for these three states revealed that, different regions of the kinase domain had different RMSF values in different phosphorylated states (Figure S4C). We observed that, while the glycine-rich loop and the αC-helix in p-IKK2 were situated in a manner reminiscent of an active kinase, those in UnP and P-IKK2 were placed very differently (Figure 4C). In fact, helix αC was found to be distorted in P-IKK2, that is unlikely to support canonical phosphotransfer from ATP. Activation segment/loop (activation loop) in these three differently phosphorylated states adopted conformations distinct from each other: activation loop in the UnP model was splayed out and moved closer to the tip of the C-lobe, whereas activation loop in p-IKK2 and P-IKK2 moved inwards and adopted conformations closer to the N-lobe (Figure 4C). The formation of the proper R- and C-spines in p-IKK2 confirmed its active form (Figure 4D). p-IKK2 KD also exhibited other canonical features of an active kinase, viz., a salt bridge between K44 and E61 (K72, E91 in PKA, respectively), 'DFG in' (DLG here) conformation. In addition, dynamic cross-correlation matrix (DCCM) or contact map of each structure suggests that specific phosphorylation events render the kinase display distinct allosteric changes at locations far from the phosphorylation sites themselves (Figure S4D).

Next, we docked ATP onto the these three phosphorylated-state structures using LeDock and GOLD followed by rescoring with AutoDock Vina using the 0 ns (starting, S) and 200ns (end, E) structures from MD simulation (see methods). It was observed that ATP binding to P-IKK2 is relatively more unfavorable (docking score in positive range) both in the starting and end structures (Figure S4E), whereas UnP and p-IKK2 binds to ATP favorably. Interestingly, each of the phospho-/unphosphorylated IKK2 species binds to ADP favorably except for the P-IKK2 in the starting conformation (Figure S4E). To look into these complexes more carefully, we extracted 50 intermediate structures from a 10 ns MD simulation and calculated binding free energies (ΔG) of these intermediate structures using the MM-PBSA

(Molecular Mechanics Poisson-Boltzmann Surface Area) method. Clearly, ATP-binding is highly unfavourable for the P-IKK2 population that has high relative preference for ADP, while p-IKK2 shows comparable preference for both (Figure S4F). Among the docked structures, ATP and its phosphate groups exhibited a pose (ΔG = -10.64 kcal/mol) (Figure S4G) very similar to that in the PKA structure (PDB ID: 1ATP), and the terminal phosphate was in close proximity to Y169-OH making autophosphorylation of Y169 highly plausible (Figure 4E). Further analyses of the ATP-bound p-IKK2 structure confirm that presence of ATP helped the R and C-spine form the desired continuum seen in the active form of a kinase (Figure 4F). Superposition of the ATP from the p-IKK2 on P-IKK2 indicated that the narrowing of canonical ATP-binding pocket in P-IKK2 may lead to rejection of ATP from the canonical binding pocket emanating from severe clashes between the glycine-rich loop and ATP (Figure 4G). However, this does not exclude the possibility of P-IKK2 employing alternative binding modes to interact with ATP. Furthermore, the R-spine in P-IKK2 was not continuous (Figure 4H), wherein M65 (L95 in PKA) of the four conserved residues were located at a position far away from the rest of three residues that constitute the R-spine, and from the glycine rich loop.

ATP binding to p-IKK2 leads to autophosphorylation at Y169 generating P-IKK2 in an ADP bound state. Interestingly, the superposition of ADP (from the docked complex of p-IKK2 and ADP, ΔG = -9.88 kCal/mol, Figure 4I) onto the P-IKK2 structure confirmed that while P-IKK2 was unable to accommodate ATP in a manner similar to that in other known experimentally derived kinase structures, it could comfortably accommodate ADP into the ATP-binding cleft (Figure 4J). It may be noted that, p-IKK2 has comparable affinities for ATP and ADP, like other kinases (Becher et al., 2013), as indicated by their respective binding energy/docking score values. Worth noting, cellular concentration of ATP and ADP plays important role in the outcome of this process where ATP concentration is much higher than ADP. We speculate that ADP-bound P-IKK2 is an intermediate step where presence of as many phosphate groups in the activation loop and ADP in such a close proximity persuades the kinase to adopt a conformation that can withstand this high density of negative charges albeit risking the integrity

of an active fold, and making some of those *de novo* phosphate groups transient in nature to return back to the p-IKK2 state to readily bind to ATP that is abound in the reaction.

These structural observations suggest that it is possible for the residues within the flexible activation segment to undergo auto-phosphorylation and possibly render the kinase with a novel phospho-transfer activity distinct from the conventional transfer of γ-phosphate from ATP to the substrate.

Freshly auto-phosphorylated IKK2 phosphorylates IκBα even in absence of ATP:

We observed phosphorylation of tyrosine residue(s) only upon fresh ATP-treatment, indicating that tyrosines of purified IKK2 loses its phosphate group during the course of purification (Eckhart et al., 1979). It may be noted that, we did not observe any density of phosphates on any of these residues in the human IKK2 crystal structure derived from ATP-treated protein sample (Polley et al., 2013). Of note, human IKK2 crystals grown with autophosphorylated IKK2 (PDB ID 4E3C) took about a month at 18-20°C before they were subjected to X-ray diffraction. This suggested an intriguing possibility that the phosphate linked to Tyr residue(s) may serve as a temporary phosphate-sink and could eventually be transferred to substrate IκBα. To test this possibility, we first allowed purified IKK2 to undergo auto-phosphorylation by incubating the excess kinase with limiting amounts of radiolabeled γ-^{32}P-ATP followed by two passes through desalting spin columns (40 kDa MW cut-off) to remove unreacted ATP. Nucleotide-free auto-phosphorylated IKK2 (P-IKK2) was incubated with IκBα either in absence of nucleotide or with newly added unlabeled nucleotides, and phosphorylation status of the substrate was subsequently monitored by autoradiography after resolving the reaction mixture on an SDS-PAGE (Figure 5A). Of note, such an experimental scheme essentially captures a single turnover phosphorylation of the substrate IκBα. Transfer of radiolabeled phosphate to IκBα was observed and the transfer was significantly enhanced in the presence of cold ADP (Figure 5B). Phosphorylation of IκBα did not significantly decrease in the presence of a high concentration of cold ATP. That addition of excess cold ATP did not reduce the extent of IκBα phosphorylation-signal on the autoradiograph strongly

suggests the transfer of ^{32}P-phosphate from ^{32}P-IKK2 to IκBα (Figure 5B) by a relay mechanism. This transfer perhaps occurs through a phosphoenzyme intermediate with or without involving ADP.

We undertook a different strategy to further confirm transfer of phosphate from the kinase (and not ATP) to the substrate. We auto-phosphorylated IKK2^{FL}-WT with excess cold ATP and removed the unreacted ATP from the reaction mixture using size-exclusion chromatography on a Superdex200 column (Figure 5C). P-IKK2 eluted at fractions corresponding to MW between 670 and 158 kDa, i.e., much larger than free ATP (Figure 5D). This P-IKK2 protein was incubated with FL IκBα either in presence or absence of ADP for different time periods. A similar reaction in presence of ATP instead of ADP was performed as a positive control. Phosphorylation of S32 and S36 (detected by the phospho-serine antibody specific to S32 and S36 of IκBα) was efficient in presence of 10 and 50 μM ADP but absent when ADP was absent in the reaction mixture. Phosphorylation of IκBα in the presence of 50 μM ATP was significantly more robust as anticipated (Figure 5E). The minor detection of IκBα phosphorylation in absence of ADP in the radioactive assay and lack of it in the cold immunoblotting assay (compare lanes marked with vertical arrows in Figures 5B and 5F) may indicate higher sensitivity of the radioactive assay. The need of ADP in phosphotransfer prompted us to consider whether the ADP was contaminated with a trace amount of ATP. ESI-MS analysis of 50 μM ADP did not detect any peak corresponding to ATP (Figure S5A). Dependence of IκBα phosphorylation on ADP could raise another possibility if microscopic reversibility generated ATP from ADP in the active site of the kinase. To this end, we employed TLC-based analysis to detect generation/presence of ATP in a similar setting as described in Figure 5A & B which revealed that no detectable ATP was present in the system, i.e., no detectable ATP was retained in the protein after passing it through the spin column twice, nor did any γP^{32}-ATP was generated when incubated with cold ADP (Figure S5B).

Phosphotransfer from P-IKK2 is critical to fidelity and specificity of IκBα phosphorylation:

We next tested if phosphotransfer is restricted only to the N-terminal signal responsive S32/S36 or to serines/threonines of the PEST domain as well. Radioactive kinase assay as described earlier was performed with full-length WT and mutant S32A, S36A (AA) IκBα as the phosphate recipient. Phosphate group(s) of P-IKK2 was not transferred to full-length IκBα AA which retains the serines and threonines within its PEST domain (Figure 6A), indicating phosphotransfer only to the N-terminal serines of IκBα that are S32 and S36. We also tested the effect of AMPPNP, an unhydrolyzable analogue of ATP, on the phosphotransfer, and found no inhibitory effect irrespective of the presence of ADP. This suggests adenine nucleotides poising the kinase for phosphotransfer (Figure 6A). A recent report proposed that IKK2 phosphorylates IκBα at S32 followed by S36 following a single binding event and that phosphorylation of S32 increases the phosphorylation rate of S36(Stephenson et al., 2022). Based on our results and other evidence, we propose that IKK2 phosphorylated at S177/S181 undergoes autophosphorylation on tyrosine residues in its activation loop area that serves as a phosphoenzyme intermediate to transfer phosphate group from IKK2 to S32 that enhances the rate of second site (S36) phosphorylation (Figure 6B). For the second site phosphorylation ATP serves as the phosphate donor.

Discussion:

We report several intriguing properties of IKK2 that contributes to its substrate phosphorylation specificity and efficiency: 1) dual specificity, involving autophosphorylation of several tyrosine residues of IKK2, in addition to known auto-phosphorylation at activation loop serines; 2) phosphate relay to the substrate IκBα via Tyr169 of auto-phosphorylated IKK2 (P-IKK2); and 3) loss of substrate specificity, despite retained catalytic activity, upon disruption of a universally conserved salt bridge mediated by Lys44.

Dual specificity of IKK2: Our present analyses of IKK2, however, revealed its surprising property wherein IKK2 phosphorylated at activation loop-serines (S177/S181) could be further auto-phosphorylated by ATP at multiple other residues yielding another form (P-IKK2) (Figure

6B). This marks IKK2 as an autocatalytic dual-specificity kinase rather than a prototype S/T kinase. This multisite phosphorylated form of IKK2 (P-IKK2) could transfer phosphate(s) to substrate IκBα in presence of ADP without requiring exogenous supply of fresh ATP (Figure 5B & E), hinting at an unusual property of IKK2 acting possibly as a phosphate-sink.

The phospho relay mechanism: Through various experimental approaches, we demonstrated that S32 of IκBα is phosphorylated via a relay mechanism. The transfer of phosphate from Tyr169 to Ser32 of IκBα represents an intriguing and unprecedented mechanism among metazoan protein kinases. We propose a plausible explanation for process: The hydroxyl group of Tyr169 is optimally positioned to readily accept the γ-phosphate from ATP at the expense of minimum energy in presence or absence of the substrate IκBα. The energy required to transfer the phosphate from Tyr169 to Ser32 is lower than that needed for a direct transfer of the same phosphate from ATP to Ser32. Thus, this relay pathway – from ATP to Tyr169 to Ser32 – might offer a more energetically favorable pathway than a direct transfer from ATP to the substrate. Another intriguing feature of phosphorelay in IKK2 is IKK2's dependence on ADP (Figure 5B & E), which the generic kinase inhibitor AMPPNP (unhydrolyzable ATP analogue) failed to inhibit (Figure 6A). Taken together, we surmise that presence of ADP or AMP-PNP helps IKK2 attain a conformational state poised for phosphorylating S32/36 of IκBα even in absence of fresh exogenous ATP. Similar phenomenon was reported for IRE1, where ADP was found to be a more potent stimulator of its ribonuclease activity and that AMPPNP could also potentiate this activity in IRE1(Lee et al., 2008; Sidrauski and Walter, 1997). We speculate that Ser32 cannot be efficiently phosphorylated by p-IKK2:ATP due to a deliberate chemical mismatch of the hydroxyl group of Ser32 within the active site. However, it aligns well with the P-IKK2:ADP intermediate. To validate this model, further structural studies and MD simulations studies are necessary. Indirect supporting evidence, as described below, underscores the existence of a unique phospho-transfer mechanism.

Tyr169 is the only residue surrounding the active site that can be involved in this relay. As phosphorylation of S32, S36 of IκBα is observed with auto-phosphorylated IKK2 EE, transferred phosphates are not from S177 or S181. Y169 is uniquely located at the DFG+1 (DLG in IKK2) position of the magnesium binding loop. This residue is exclusive to IKK1 and IKK2 and is absent even in close mammalian homologues, IKKε and TBK1. Notably, neither IKKε nor TBK1 can phosphorylate IκBα at S32 and S36, either *in vitro* or *in vivo*(Larabi et al., 2013; Tu et al., 2013) supporting the assertion that the phospho-transfer is a genuine and specific event. Recent findings suggest that the DFG+1 residue plays a critical in distinguishing Ser versus Thr residues (Chen et al., 2014). These observations highlight the dual role of Y169 in both substrate selectivity and catalytic activity. This dual selectivity – at residue level (serine versus threonine) and the catalytic level (mediated by relay Tyr169) underpins the exquisite specificity of IκBα for the IKK. Additional mechanisms, such as conformational changes associated with Tyr169 phosphorylation may further enhance the efficiency of the relay by properly positioning Ser32 for phospho-transfer. It is worthwhile to note that, a phospho-resistant mutation at S32 in IκBα to Ile (S32I) is associated with ectodermal dysplasia and T-cell immunodeficiency in patients(Courtois et al., 2003; Mooster et al., 2015). To the best of our knowledge, it is the first report, apart from MHCK of *Dictyostelium discoideum* (an atypical EPK), to suggest that a metazoan EPK confirms its specificity through the formation of a phosphoenzyme intermediate(Ye et al., 2010).

Tyrosine residues within the activation loop of IKK2 have been previously reported to undergo signal-induced phosphorylation in cells. Although these modifications were proposed to be mediated by a tyrosine kinase, no specific tyrosine kinase has been identified to date(Meyer et al., 2013; Otero et al., 2008; Rieke et al., 2011). Notably, several members of the Ser/Thr kinase family are known to undergo tyrosine phosphorylation, employing diverse mechanisms for autophosphorylation (Bhattacharyya et al., 2006; Ge et al., 2002; Lochhead, 2009; Lochhead et al., 2006, 2005; Tigno-Aranjuez et al., 2010). Regardless of the mechanism

responsible for Tyr169 phosphorylation, the phosphate attached to Tyr169 is uniquely primed for transfer to Ser32 of IκBα.

Allostery in phosphorylation: Several other residues, including tyrosines distributed throughout the kinase molecule, also undergo phosphorylation. While most of these phosphorylations play a role in global stabilization of the kinase, Tyr188 plays a critical role in substrate phosphorylation. Mutation of Tyr188—a conserved tyrosine residue—to a non-phosphorylatable phenylalanine completely abolished IKK2 kinase activity both *in vitro* and in MEF cells following TNF treatment (Figure 3E & G). The structural placement of Tyr188 suggests that its mutation may allosterically disrupt kinase activity, making its precise role in phosphotransfer unclear. Autophosphorylation of kinase domains is a well-documented regulatory mechanism in other kinases as well. For example, autophosphorylation at Thr220 significantly impacts both the activity and substrate specificity of CK1 (Cullati et al., 2022).

Signaling specificity and digital activation: The strength of the input signal, along with the extent of IκBα degradation and NF-κB activation, is closely associated with the amplitude, duration, and kinetics of IKK activity (Behar and Hoffmann, 2013; Cheong et al., 2006). The digital (all-or-none) activation profile of NF-κB appears to arise from the rapid activation and inactivation dynamics of IKK2. While IKK phosphorylates multiple substrates in vivo, the swift activation of NF-κB is predominantly governed by IκBα, with IκBβ and IκBε playing lesser roles. This digital activation profile may be intrinsically linked to the phosphate relay process. We propose that Tyr169 serves as both a selection mechanism and a mediator of the rapid phosphorylation kinetics.

Interestingly, the regulatory system of IKK2 may be somewhat analogous to the two-component histidine kinase-effector systems in prokaryotes, which exhibit threshold activation responses (Bhate et al., 2015; Lamarche et al., 2008; Laub and Goulian, 2007). It is noteworthy that phosphate transfer directly from pHis is energetically far more favorable than from pTyr, except in enzymatic processes. However, Tyr169 might be special case, behaving similar to active site His in histidine kinases.

The conserved salt bridge is specificity determinant not activity. Our study highlights the role of K44 in IKK2 autophosphorylation, which is crucial for the specific phosphorylation of Ser32 and Ser36 of IκBα. Interestingly, while the K44 mutant retains non-specific kinase activity, its phosphorylation specificity is compromised. Notably, a monomeric form of IKK2, lacking the NBD and a large portion of the dimeric interface in the SDD, maintains specificity for the N-terminal serines of IκBα (Hauenstein et al., 2014). However, a truncated construct containing only the KD and ULD loses this specificity, behaving like CK2 and phosphorylating the PEST domain (Shaul et al., 2008). Further studies are needed to determine whether a specific structural state of IKK2, possibly influenced by alternative modifications or interactions with other proteins, enables non-specific substrate phosphorylation.

Conclusion: In all, it is intriguing how the gateway to the activation of NF-κB is regulated through unique phosphorylation events in IKK2. It appears that a multi-layered fail-safe mechanism is devised to tightly control NF-κB activation. In absence of upstream signals, the IKK-complex is unable to phosphorylate Ser 32,36 of IκBα efficiently thereby keeping check on the aberrant and untimely activation of NF-κB. Upon encountering proinflammatory cues, cells need to activate NF-κB immediately, efficiently and specifically, i.e., IKK needs to be activated and phosphorylate Ser 32,36 of IκBα. NEMO warrants IKK-activation and ensures that the IKK-complex specifically chooses IκBα from a large pool of substrates of IKK2. IKK2 is designed in such a manner that it phosphorylates itself at activation loop-tyrosine when activated, such that phosphate group(s) can be relayed directly to Ser32,36 of IκBα with great fidelity, thus leaving little chance of a misconstrued signaling event thereby confirming NF-κB activation. Our discovery might also present the beginning of a new aspect in eukaryotic cell-signaling by EPKs and provide a foundation for mechanistic studies of an intriguing phospho-transfer reaction that helps accomplish the desired specificity.

Methods summary:

Protein purification, auto-phosphorylation assay, immunoprecipitation coupled kinase assay, phosphotransfer assay and other experiments have been described in details in the supplementary document.

Acknowledgement:

We thank Tony Hunter (Salk Institute) and Kaushik Biswas (BI) for commenting on the work. Authors also thank members of Polley lab (BI) and Ghosh Lab (UCSD) for their continuous support. This work was supported by an Intermediate Fellowship from the DBT Wellcome Trust India Alliance (IA/I/15/1/501852) & intramural funding from Bose Institute to SP, NIH grant to GG (AI163327) and American Cancer Society grant RSG-08-287-01-GMC to TH. Biochemistry research at SDSU is supported in part by the California Metabolic Research Foundation. PB was supported by the graduate research fellowship from Bose Institute. SC acknowledges CSIR-IICB for infrastructure support. AC acknowledges ICMR for post-doctoral Research Associateship [BMI/11(55)2022].

Author contribution:

SP, GG and TB designed experiments; PB, SP, TB & GG performed experiments. Computational analyses were performed by AC & SC. SP, GG, TB, PB, TH, SC and AC analyzed the results. SP wrote the manuscript with the help of PB, TB and AC in preparing figures and images. GG, TB, PB and TH edited/modified the manuscript. All authors commented on the manuscript.

Ethics declarations:

Competing interests: The authors declare no competing financial interests.

References:

Ahuja LG, Kornev AP, McClendon CL, Veglia G, Taylor SS. 2017. Mutation of a kinase allosteric node uncouples dynamics linked to phosphotransfer. *Proc Natl Acad Sci U S A* **114**:E931–E940. doi:10.1073/pnas.1620667114

Antonia RJ, Hagan RS, Baldwin AS. 2021. Expanding the View of IKK: New Substrates and New Biology. *Trends Cell Biol* **31**:166–178. doi:10.1016/j.tcb.2020.12.003

Barroga CF, Stevenson JK, Schwarz EM, Verma IM. 1995. Constitutive phosphorylation of I kappa B alpha by casein kinase II. *Proceedings of the National Academy of Sciences* **92**:7637–7641. doi:10.1073/pnas.92.17.7637

Becher I, Savitski MM, Savitski MF, Hopf C, Bantscheff M, Drewes G. 2013. Affinity profiling of the cellular kinome for the nucleotide cofactors ATP, ADP, and GTP. *ACS Chem Biol* **8**:599–607. doi:10.1021/cb3005879

Behar M, Hoffmann A. 2013. Tunable Signal Processing through a Kinase Control Cycle: the IKK Signaling Node. *Biophys J* **105**:231–241. doi:10.1016/j.bpj.2013.05.013

Bhate MP, Molnar KS, Goulian M, DeGrado WF. 2015. Signal Transduction in Histidine Kinases: Insights from New Structures. *Structure* **23**:981–994. doi:10.1016/j.str.2015.04.002

Bhattacharyya RP, Reményi A, Good MC, Bashor CJ, Falick AM, Lim WA. 2006. The Ste5 scaffold allosterically modulates signaling output of the yeast mating pathway. *Science* **311**:822–826. doi:10.1126/science.1120941

Brown K, Gerstberger S, Carlson L, Franzoso G, Siebenlist U. 1995. Control of I kappa B-alpha proteolysis by site-specific, signal-induced phosphorylation. *Science* **267**:1485–1488. doi:10.1126/science.7878466

Chen C, Ha BH, Thevenin AF, Lou HJ, Zhang R, Yip KY, Peterson JR, Gerstein M, Kim PM, Filippakopoulos P, Knapp S, Boggon TJ, Turk BE. 2014. Identification of a major determinant for serine-threonine kinase phosphoacceptor specificity. *Mol Cell* **53**:140–7. doi:10.1016/j.molcel.2013.11.013

Chen ZJ. 2012. Ubiquitination in Signaling to and Activation of IKK. *Immunol Rev* **246**:95–106. doi:10.1111/j.1600-065X.2012.01108.x

Cheong R, Bergmann A, Werner SL, Regal J, Hoffmann A, Levchenko A. 2006. Transient IkappaB kinase activity mediates temporal NF-kappaB dynamics in response to a wide range of tumor necrosis factor-alpha doses. *J Biol Chem* **281**:2945–50. doi:10.1074/jbc.M510085200

Courtois G, Smahi A, Reichenbach J, Döffinger R, Cancrini C, Bonnet M, Puel A, Chable-Bessia C, Yamaoka S, Feinberg J, Dupuis-Girod S, Bodemer C, Livadiotti S, Novelli F, Rossi P, Fischer A, Israël A, Munnich A, Le Deist F, Casanova J-L. 2003. A hypermorphic IkappaBalpha mutation is associated with autosomal dominant anhidrotic ectodermal dysplasia and T cell immunodeficiency. *J Clin Invest* **112**:1108–1115. doi:10.1172/JCI18714

Cullati SN, Chaikuad A, Chen J-S, Gebel J, Tesmer L, Zhubi R, Navarrete-Perea J, Guillen RX, Gygi SP, Hummer G, Dötsch V, Knapp S, Gould KL. 2022. Kinase domain autophosphorylation rewires the activity and substrate specificity of CK1 enzymes. *Mol Cell* **82**:2006-2020.e8. doi:10.1016/j.molcel.2022.03.005

Darwech I, Otero JE, Alhawagri MA, Abu-Amer Y. 2010. Tyrosine phosphorylation is required for IkappaB kinase-beta (IKKbeta) activation and function in osteoclastogenesis. *J Biol Chem* **285**:25522–25530. doi:10.1074/jbc.M110.121533

Delhase M, Hayakawa M, Chen Y, Karin M. 1999. Positive and Negative Regulation of IκB Kinase Activity Through IKKβ Subunit Phosphorylation. *Science* **284**:309–313. doi:10.1126/science.284.5412.309

DiDonato JA, Hayakawa M, Rothwarf DM, Zandi E, Karin M. 1997. A cytokine-responsive IκB kinase that activates the transcription factor NF-κB. *Nature* **388**:548–554. doi:10.1038/41493

Du M, Ea CK, Fang Y, Chen ZJ. 2022. Liquid phase separation of NEMO induced by polyubiquitin chains activates NF-kappaB. *Mol Cell* **82**:2415-2426 e5. doi:10.1016/j.molcel.2022.03.037

Ea CK, Deng L, Xia ZP, Pineda G, Chen ZJ. 2006. Activation of IKK by TNFalpha requires site-specific ubiquitination of RIP1 and polyubiquitin binding by NEMO. *Mol Cell* **22**:245–57. doi:10.1016/j.molcel.2006.03.026

Eckhart W, Hutchinson MA, Hunter T. 1979. An activity phosphorylating tyrosine in polyoma T antigen immunoprecipitates. *Cell* **18**:925–933. doi:10.1016/0092-8674(79)90205-8

Ge B, Gram H, Di Padova F, Huang B, New L, Ulevitch RJ, Luo Y, Han J. 2002. MAPKK-independent activation of p38alpha mediated by TAB1-dependent autophosphorylation of p38alpha. *Science* **295**:1291–1294. doi:10.1126/science.1067289

Ghosh S, Karin M. 2002. Missing pieces in the NF-kappaB puzzle. *Cell* **109 Suppl**:S81-96.

Hacker H, Karin M. 2006. Regulation and function of IKK and IKK-related kinases. *Sci STKE* **2006**:re13. doi:10.1126/stke.3572006re13

Hauenstein AV, Rogers WE, Shaul JD, Huang DB, Ghosh G, Huxford T. 2014. Probing kinase activation and substrate specificity with an engineered monomeric IKK2. *Biochemistry* **53**:2064–73. doi:10.1021/bi401551r

Hayden MS, Ghosh S. 2008. Shared principles in NF-kappaB signaling. *Cell* **132**:344–62. doi:10.1016/j.cell.2008.01.020

Hinz M, Scheidereit C. 2014. The IκB kinase complex in NF-κB regulation and beyond. *EMBO Rep* **15**:46–61. doi:10.1002/embr.201337983

Hoffmann A, Baltimore D. 2006. Circuitry of nuclear factor kappaB signaling. *Immunol Rev* **210**:171–86. doi:10.1111/j.0105-2896.2006.00375.x

Huse M, Kuriyan J. 2002. The conformational plasticity of protein kinases. *Cell* **109**:275–282. doi:10.1016/s0092-8674(02)00741-9

Karin M, Ben-Neriah Y. 2000. Phosphorylation meets ubiquitination: the control of NF-[kappa]B activity. *Annu Rev Immunol* **18**:621–63. doi:10.1146/annurev.immunol.18.1.621

Knighton DR, Zheng JH, Ten Eyck LF, Xuong NH, Taylor SS, Sowadski JM. 1991. Structure of a peptide inhibitor bound to the catalytic subunit of cyclic adenosine monophosphate-dependent protein kinase. *Science* **253**:414–420. doi:10.1126/science.1862343

Lamarche MG, Wanner BL, Crépin S, Harel J. 2008. The phosphate regulon and bacterial virulence: a regulatory network connecting phosphate homeostasis and pathogenesis. *FEMS Microbiol Rev* **32**:461–473. doi:10.1111/j.1574-6976.2008.00101.x

Larabi A, Devos JM, Ng SL, Nanao MH, Round A, Maniatis T, Panne D. 2013. Crystal structure and mechanism of activation of TANK-binding kinase 1. *Cell Rep* **3**:734–46. doi:10.1016/j.celrep.2013.01.034

Laub MT, Goulian M. 2007. Specificity in two-component signal transduction pathways. *Annu Rev Genet* **41**:121–45. doi:10.1146/annurev.genet.41.042007.170548

Lee KPK, Dey M, Neculai D, Cao C, Dever TE, Sicheri F. 2008. Structure of the dual enzyme Ire1 reveals the basis for catalysis and regulation in non-conventional RNA splicing. *Cell* **132**:89–100. doi:10.1016/j.cell.2007.10.057

Lin YC, Brown K, Siebenlist U. 1995. Activation of NF-kappa B requires proteolysis of the inhibitor I kappa B-alpha: signal-induced phosphorylation of I kappa B-alpha alone does not release active NF-kappa B. *Proceedings of the National Academy of Sciences* **92**:552–556. doi:10.1073/pnas.92.2.552

Liu F, Xia Y, Parker AS, Verma IM. 2012. IKK biology. *Immunol Rev* **246**:239–53. doi:10.1111/j.1600-065X.2012.01107.x

Liu S, Misquitta YR, Olland A, Johnson MA, Kelleher KS, Kriz R, Lin LL, Stahl M, Mosyak L. 2013. Crystal Structure of a Human IκB Kinase β Asymmetric Dimer. *J Biol Chem* **288**:22758–22767. doi:10.1074/jbc.M113.482596

Lochhead PA. 2009. Protein kinase activation loop autophosphorylation in cis: overcoming a Catch-22 situation. *Sci Signal* **2**:pe4. doi:10.1126/scisignal.254pe4

Lochhead PA, Kinstrie R, Sibbet G, Rawjee T, Morrice N, Cleghon V. 2006. A chaperone-dependent GSK3beta transitional intermediate mediates activation-loop autophosphorylation. *Mol Cell* **24**:627–633. doi:10.1016/j.molcel.2006.10.009

Lochhead PA, Sibbet G, Morrice N, Cleghon V. 2005. Activation-loop autophosphorylation is mediated by a novel transitional intermediate form of DYRKs. *Cell* **121**:925–936. doi:10.1016/j.cell.2005.03.034

Meyer AN, Drafahl KA, McAndrew CW, Gilda JE, Gallo LH, Haas M, Brill LM, Donoghue DJ. 2013. Tyrosine Phosphorylation Allows Integration of Multiple Signaling Inputs by IKKβ. *PLoS One* **8**:e84497. doi:10.1371/journal.pone.0084497

Mooster JL, Le Bras S, Massaad MJ, Jabara H, Yoon J, Galand C, Heesters BA, Burton OT, Mattoo H, Manis J, Geha RS. 2015. Defective lymphoid organogenesis underlies the immune deficiency caused by a heterozygous S32I mutation in IκBα. *J Exp Med* **212**:185–202. doi:10.1084/jem.20140979

Nolen B, Taylor S, Ghosh G. 2004. Regulation of Protein Kinases: Controlling Activity through Activation Segment Conformation. *Molecular Cell* **15**:661–675. doi:10.1016/j.molcel.2004.08.024

Otero JE, Dai S, Foglia D, Alhawagri M, Vacher J, Pasparakis M, Abu-Amer Y. 2008. Defective osteoclastogenesis by IKKbeta-null precursors is a result of receptor activator of NF-kappaB ligand (RANKL)-induced JNK-dependent apoptosis and impaired differentiation. *J Biol Chem* **283**:24546–24553. doi:10.1074/jbc.M800434200

Polley S, Huang D-B, Hauenstein AV, Fusco AJ, Zhong X, Vu D, Schröfelbauer B, Kim Y, Hoffmann A, Verma IM, Ghosh G, Huxford T. 2013. A structural basis for IκB kinase 2 activation via oligomerization-dependent trans auto-phosphorylation. *PLoS Biol* **11**:e1001581. doi:10.1371/journal.pbio.1001581

Rieke C, Papendieck A, Sokolova O, Naumann M. 2011. Helicobacter pylori-induced tyrosine phosphorylation of IKKβ contributes to NF-κB activation. *Biol Chem* **392**:387–393. doi:10.1515/BC.2011.029

Robbins DJ, Zhen E, Owaki H, Vanderbilt CA, Ebert D, Geppert TD, Cobb MH. 1993. Regulation and properties of extracellular signal-regulated protein kinases 1 and 2 in vitro. *J Biol Chem* **268**:5097–106.

Rothwarf DM, Zandi E, Natoli G, Karin M. 1998. IKK-gamma is an essential regulatory subunit of the IkappaB kinase complex. *Nature* **395**:297–300. doi:10.1038/26261

Scheidereit C. 2006. IkappaB kinase complexes: gateways to NF-kappaB activation and transcription. *Oncogene* **25**:6685–705. doi:10.1038/sj.onc.1209934

Schrofelbauer B, Hoffmann A. 2011. How do pleiotropic kinase hubs mediate specific signaling by TNFR superfamily members? *Immunol Rev* **244**:29–43. doi:10.1111/j.1600-065X.2011.01060.x

Schröfelbauer B, Polley S, Behar M, Ghosh G, Hoffmann A. 2012. NEMO ensures signaling specificity of the pleiotropic IKKβ by directing its kinase activity toward IκBα. *Mol Cell* **47**:111–121. doi:10.1016/j.molcel.2012.04.020

Shaul JD, Farina A, Huxford T. 2008. The human IKKbeta subunit kinase domain displays CK2-like phosphorylation specificity. *Biochem Biophys Res Commun* **374**:592–7. doi:10.1016/j.bbrc.2008.07.082

Sidrauski C, Walter P. 1997. The transmembrane kinase Ire1p is a site-specific endonuclease that initiates mRNA splicing in the unfolded protein response. *Cell* **90**:1031–1039. doi:10.1016/s0092-8674(00)80369-4

Stephenson AA, Taggart DJ, Xu G, Fowler JD, Wu H, Suo Z. 2022. The inhibitor of κB kinase β (IKKβ) phosphorylates IκBα twice in a single binding event through a sequential mechanism. *J Biol Chem* **299**:102796. doi:10.1016/j.jbc.2022.102796

Tergaonkar V, Bottero V, Ikawa M, Li Q, Verma IM. 2003. IkappaB kinase-independent IkappaBalpha degradation pathway: functional NF-kappaB activity and implications for cancer therapy. *Mol Cell Biol* **23**:8070–83.

Tigno-Aranjuez JT, Asara JM, Abbott DW. 2010. Inhibition of RIP2's tyrosine kinase activity limits NOD2-driven cytokine responses. *Genes Dev* **24**:2666–2677. doi:10.1101/gad.1964410

Tu D, Zhu Z, Zhou AY, Yun CH, Lee KE, Toms AV, Li Y, Dunn GP, Chan E, Thai T, Yang S, Ficarro SB, Marto JA, Jeon H, Hahn WC, Barbie DA, Eck MJ. 2013. Structure and

ubiquitination-dependent activation of TANK-binding kinase 1. *Cell Rep* **3**:747–58. doi:10.1016/j.celrep.2013.01.033

Xu G, Lo Y-C, Li Q, Napolitano G, Wu X, Jiang X, Dreano M, Karin M, Wu H. 2011. Crystal structure of inhibitor of κB kinase β (IKKβ). *Nature* **472**:325–330. doi:10.1038/nature09853

Yang J, Garrod SM, Deal MS, Anand GS, Woods VL Jr, Taylor S. 2005. Allosteric network of cAMP-dependent protein kinase revealed by mutation of Tyr204 in the P+1 loop. *J Mol Biol* **346**:191–201. doi:10.1016/j.jmb.2004.11.030

Ye Q, Crawley SW, Yang Y, Côté GP, Jia Z. 2010. Crystal structure of the alpha-kinase domain of Dictyostelium myosin heavy chain kinase A. *Sci Signal* **3**:ra17. doi:10.1126/scisignal.2000525

Zandi E, Chen Y, Karin M. 1998. Direct phosphorylation of IkappaB by IKKalpha and IKKbeta: discrimination between free and NF-kappaB-bound substrate. *Science* **281**:1360–1363. doi:10.1126/science.281.5381.1360

Zandi E, Rothwarf DM, Delhase M, Hayakawa M, Karin M. 1997. The IkappaB kinase complex (IKK) contains two kinase subunits, IKKalpha and IKKbeta, necessary for IkappaB phosphorylation and NF-kappaB activation. *Cell* **91**:243–252. doi:10.1016/s0092-8674(00)80406-7

Zhang J, Clark K, Lawrence T, Peggie MW, Cohen P. 2014. An unexpected twist to the activation of IKKbeta: TAK1 primes IKKbeta for activation by autophosphorylation. *Biochem J* **461**:531–7. doi:10.1042/BJ20140444

Figure legends:

Figure 1: Autophosphorylation of IKK2 at hitherto uncharacterized sites. (A) NEMO is known to remain bound to the IKK-complex pre- and post-stimulation, helps in activation as well as substrate recognition to channelize IKK-activity towards IκBα. However, it is not clear how IKK specifically phosphorylates the Ser32&36 of IκBα. **(B)** Domain organisation of FL IKK2 depicting functional kinase domain (KD), ubiquitin-like domain (ULD), and scaffold dimerization domain (SDD) based on the X-ray structures. Known sites of Ser phosphorylation and NEMO interacting regions at the extreme C-termini are highlighted. Serine and tyrosine residues in the activation loop are shown, mutation of which to Glu renders IKK2 constitutively active. The conserved ATP-interacting Lys (at position 44) is also shown. **(C)** Autophosphorylation of FL IKK2WT upon incubation with radioactive ATP for different time periods in an *in vitro* kinase assay. **(D)** *In vitro* radioactive kinase assays performed to check the effect of NEMO on autophosphorylation of FL IKK2WT (left panel), and that of NEMO and IκBα on autophosphorylation and substrate phosphorylation (right panel) activity of FL IKK2WT. **(E)** Effect of Inhibitor VII on FL IKK2WT autophosphorylation and IκBα substrate phosphorylation at different inhibitor concentrations in a radioactive *in vitro* kinase assay. A schematic representation of the assay procedure is shown in Figure S1B. This assay was performed twice. **(F)** Radioactive kinase assay conducted to check auto- and substrate phosphorylation of full length and deletion constructs of constitutively active form of IKK2 harbouring phosphomimetic Ser177Glu and Ser181Glu mutations.

Figure 2: IKK2 possesses autocatalytic dual specificity. (A) *In vitro* kinase assay, followed by immunoblotting with FL IKK2WT using antibodies against phosphor-Ser (177/181) and phospho-Tyr. **(B)** A different commercial source of phospho-Tyr antibody was used to detect pTyr on IKK2. **(C)** Effect of Inhibitor VII on tyrosine autophosphorylation of FL IKK2WT. **(D)** Immunoblotting performed with phospho-Tyr antibody to check autophosphorylation of IKK2 mutant K44M at different time points compared to that of IKK2 WT. **(E)** Tyrosine autophosphorylation and substrate phosphorylation of GST (1-54) IκBα in presence of full length and deletion mutants of IKK2 harbouring phosphomimetic Ser177Glu and Ser181Glu mutations. **(F)** *De novo* auto-phosphorylation of IKK2 on tyrosine monitored by phospho-Ser and phospho-Tyr specific monoclonal antibodies. **(G)** Autophosphorylation and subsequent immunoblot analysis of FLIKK2 mutant S177A, S181A using antibodies against phospho-IKK2-Ser(177/181) and phospho-Tyr.

Figure 3: Dual-specific autophosphorylation is critical for IKK2's function: (A) Position of canonically important residues in the AL (purple ribbon) of IKK2-KD are shown in the context of its structure (PDB ID 4E3C; surface representation; KD is shown light green with respect to the SDD in teal). Autophosphorylated tyrosine residues identified in this study are shown in green. (B) Alignment of the activation segment sequences of different IKK family kinases. Conservation of Tyr at the DFG+1 (DLG in case of IKK1 and IKK2) is retained only in a stress response related plant kinase SnRK2, but not in other IKK homologues or any known dual specificity kinases, e.g., DYRK and GSK3β (both contain Ser at that position). Tyr188 (204 in PKA) is conserved. **(C)** Comparison of substrate and autophosphorylation activities of FL IKK2 WT and K44M mutant in an *in vitro* radioactive kinase assay performed with or without FL IκBα WT as the substrate. **(D)** Residue level specificity of phosphorylation by the FL IKK2 K44M was analysed using an antibody that specifically recognizes phospho-S32/36 of IκBα. **(E)** Radioactive *in vitro* kinase assay performed with IKK2 Y169F and Y188F mutants using GST (1-54) IκBα WT and AA as substrates. **(F)** Radioactive *in vitro* kinase assay performed with IKK2 Y169F mutant with a range of GST (1-54) IκBα mutants where the substrate phosphorylation signal is abolished in case of S36 A/E IκBα. **(G)** Severe reduction in TNFα-induced IKK activity in *ikk2-/-* MEF-3T3 cells reconstituted with mutant (Y169F and Y188F) IKK2s compared to wild-type. Kinase assay was performed with IKK immunoprecipitated (IP-ed) with anti-NEMO antibody from whole cell extract (n=2).

Figure 4: Structural analyses of IKK2 autophosphorylation. (A) Molecular dynamics (MD) simulations of all three differently phosphorylated states of IKK2 was performed. 200ns trajectory of energy for each state is shown in golden yellow, blue and copper red representing UnP-IKK2, p-IKK2 and P-IKK2, respectively. Same color coding has been followed throughout this figure and the corresponding supplementary figure. **(B)** 200ns trajectory of RMSD for each state is shown**. (C)** Residues forming canonical R- (labelled in blue) & C-spines (labelled in dark gray) representative of an active conformation in p-IKK2 are shown. **(D)** Superposition of structures representing the differently phosphorylated states post 200ns MD simulation. Relevant sections, e.g., activation loop, αC-helix, Gly-rich loop areas are highlighted in the right panel. **(E)** ATP-bound p-IKK2 structure is depicted. In the right panel, relevant residues are highlighted. Y169 is found in a position poised for autophosphorylation. **(F)** ATP completes the desired continuum of R- & C-spine observed in active kinase conformations. **(G)** P-IKK2 cannot accommodate ATP in its cleft, and αC-helix is displaced. **(H)** M is moved away from the R-spine, failing to form canonically active conformation of R- & C-spines. **(I & J)** ADP-bound p-IKK2 and P-IKK2 states are shown, respectively. Both p-IKK2 and P-IKK2 states can accommodate ADP in their respective clefts.

Figure 5: Freshly autophosphorylated IKK2 relays phosphates to IκBα. (A) Schematic representation of the experiment performed to monitor the path traversed by phosphate(s) from phospho-IKK2 to substrate by autoradiography detection method. **(B)** Purified autophosphorylated (radiolabelled) IKK2 transfers its phosphate to IκBα substrate in absence of any nucleotide, and transfer efficiency is enhanced upon addition of ADP or ATP. **(C)** Schematic representation of the experiment performed to monitor the path traversed by phosphate(s) from phospho-IKK2 to substrate by immunoblotting detection method. **(D)** Elution profile of the size exclusion chromatography run of phospho-IKK2 to get rid of excess unlabelled ATP performed in Superdex200 10/30 increase. **(E)** Purified autophosphorylated (cold) IKK2 transfers its phosphate to IκBα substrate with enhanced transfer efficiency upon addition of ADP or ATP monitored by immunoblotting using specific antibodies as indicated in the figure.

Figure 6: Specificity and fidelity of phosphotransfer by IKK2 to IκBα. (**A**) AMP-PNP can support efficient phosphotransfer. Also, phosphotransfer is observed in IκBα WT but not in S32,36Ala double mutant. Domain organization and position of relevant S/T/Y residues of IκBα are shown above the autoradiograph. **(B)** A detailed scheme of reactions showing IKK2-activation and subsequent phosphorylation of the signal responsive S32,36 on IκBα by phosphotransfer in presence of ADP.

Figure Supplement 1: (A) Autoradiograph of *in vitro* kinase assay reactions carried out with FL IKK2 WT and K44M using GST (1-54) IκBα as the substrate as a function of time. **(B)** Effect of Inhibitor VII on FL IKK2WT autophosphorylation and IκBα substrate phosphorylation specifically on S32/36 at different inhibitor concentrations in a non-radioactive *in vitro* kinase assay monitored using a monoclonal antibody that specifically recognizes IκBα phosphorylated at those two serines. A scheme of kinase assays done to check the effect of the inhibitors is shown in the box below the gel image. **(C)** Coomassie stained SDS-PAGE showing purity of some of the IKK2 proteins used in this study (Left panel). Silver stained SDS-PAGE of 3 different versions of IKK2 proteins. **(D)** LC MS/MS analyses of FL IKK2 K44M protein after Trypsin digestion on Orbitrap Exploris™ 240 equipment. A 3D scatter plot with different parameters for the detected proteins obtained from the mass spectrometric analysis of the sample is shown, where X-axis represents no. of unique peptides for each protein, Y-axis represents spectral counts and Z-axis represents the iBAQ (intensity Based Absolute Quantification) values. In the left panel all the proteins detected are shown where orange circle represents the protein kinases, whereas in the right panel only the protein kinases are shown.

For this analysis *Spodoptera frugiperda* reference proteome (ID: UP000829999) available in Uniprot database was used that contains both reviewed and unreviewed proteins.

Figure Supplement 2: (A) Effect of increasing concentration of urea on tyrosine autophosphorylation of FL IKK2WT assessed in an *in vitro* kinase assay monitored by immunoblotting. **(B)** Radioactive *in vitro* kinase assay performed with increasing concentration of urea up to 6M to check auto- and substrate phosphorylation. **(C)** Inhibition of both substrate phosphorylation and tyrosine autophosphorylation activities of IKK2 checked in presence of common kinase inhibitors such as AMPPNP and Staurosporine, highly specific IKK2 inhibitors TPCA, Calbiochem Inhibitor VII and MLN120B. **(D)** Mutation of AL-serines to non-phosphorylatable alanine (FL IKK2 S177A,181A double mutant) debilitates its kinase activity towards S32,36 of IκBα compared to WT or EE version of IKK2 as observed in an *in vitro* kinase assay.

Figure Supplement 3: (A) LC MS/MS based detection of phosphorylated tyrosine residues (Y169, Y325 and Y188, from left to right) on autophosphorylated FL IKK2 WT. **(B)** A close-up view of the active site in active form in the context of the entire kinase domain of IKK2. Three tyrosines (Y169, Y188 and Y199) in immediate vicinity of active sites are highlighted. Position of ATP is modelled based on the structure of PKA. **(C)** Substrate bound PKA in its active form; phosphorylatable serine of the substrate peptide (in magenta) is highlighted. **(D)** Immunoblotting performed with phospho-IKK2 Ser(177/181) antibody to check autophosphorylation of IKK2 mutant K44M at different time points compared to that of IKK2 WT. **(E)** Differential sensitivity of specific vs. non-specific phosphorylation by IKK2 as assessed by the effect of Inhibitor VII on FL IKK2 WT and IKK2 K44M using IκBα WT and AA as substrates. **(F)** To compare the effect of Y169F mutation on phosphorylation of S32 and S36 of IκBα with respect to FL IKK2 WT, similar assay as described in Figure 3F was performed. Reactions with Y169F were performed exactly the same way as with the WT kinase. Reactions with IKK2 WT were run on a single gel, whereas that with Y169F were run on a different gel. They were processed exactly the same way and exposed for autoradiography before imaging (n=1). **(G)** AL-serine phosphorylation status of IKK2 WT and Y169F was assessed in reconstituted MEFs post-stimulation with TNF-α after immunoprecipitating the kinase with monoclonal anti-HA antibody (n=2).

Figure Supplement 4: (A) A differential scanning calorimetry (DSC) thermogram showing a striking enhancement in folding stability of IKK2 upon ATP-treatment. **(B)** Ribbon representation of different phosphorylated versions of IKK2 are shown: UnP-IKK2 in golden

yellow, p-IKK2 in blue and P-IKK2 in copper red. **(C)** Trajectories of RMSF for these structures are shown (left panel). For clarity, different regions of the KD are shown in the right. **(D)** Dynamic cross-correlation matrix (DCCM) or contact map of each structure reveals phosphorylation-induced local as well as allosteric changes. **(E)** Docking scores of ATP and ADP bound to differently phosphorylated IKK2 proteins using three different docking programs. ATP and ADP were docked to respective IKK2 models at 0ns at 200ns of MD simulation using LeDock and GOLD followed by rescoring with AutoDock Vina (see methods). **(F)** Percentage of unfavorable poses having $\Delta G>0$ obtained from MM-PBSA (Molecular Mechanics Poisson-Boltzmann Surface Area) method for each phosphorylated state of IKK2 using 50 intermediate complex structures in a 10ns MD simulation of respective complex structures post-docking (see methods). **(G)** ATP-bound structure of p-IKK2 (ribbon) is shown.

Figure Supplement 5: (A) ESI-MS scan of the ADP used in this assay system showing negligible trace, if any, of ATP at 50μM ADP concentration. **(B)** Regeneration of ATP, if any, through microscopic reversibility was checked by TLC in a variety of conditions. γ-P^{32} was used as the control/standard. **(C)** Quantitation of phospho-IκBα (at Ser32/36) and tyrosine phosphorylated IKK2 from Figure 5E. Quantitation of the bands was done using ImageQuant TL software. The average intensity values were first normalized, and then the ratio of the normalized average intensity of the phosphorylated protein with their respective whole protein controls was plotted using Microsoft Excel. **(D)** Transfer of phosphates from purified autophosphorylated (cold) IKK2 to IκBα substrate increases in a time dependent manner in presence of a fixed concentration of ADP. Progress of the reaction is monitored by immunoblotting using specific antibodies as indicated in the figure (n=2).

Figure Supplement 6: Purified autophosphorylated (radiolabelled) FL IKK2 Y69F fails to transfer phosphate to IκBα substrate in presence or absence of ADP (n=1). The assay was performed using the same scheme as described in Figure 5A.

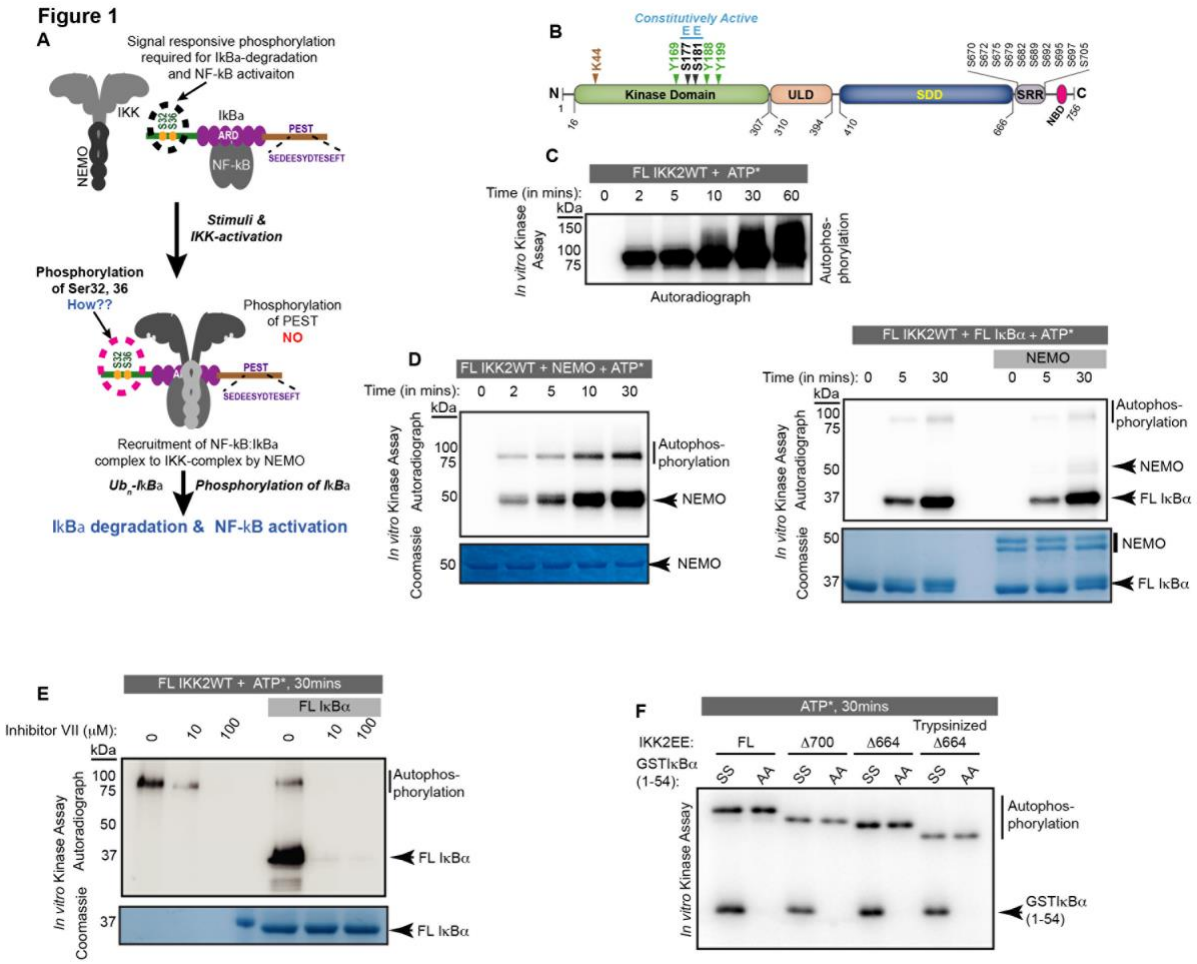
Figure 1
A
Signal responsive phosphorylation required for IkBa-degradation and NF-kB activaiton
IKK
IkBa
NEMO
NF-kB
PEST
ARD
SEDEESYDTESEFT
Stimuli & IKK-activation
Phosphorylation of Ser32, 36
How??
Phosphorylation of PEST
NO
Recruitment of NF-kB:IkBa complex to IKK-complex by NEMO
Ubn-IkBa
Phosphorylation of IkBa
IkBa degradation & NF-kB activation
B
Constitutively Active
E E
K44
Y169
S177
S181
Y188
Y199
N
C
Kinase Domain
ULD
SDD
SRR
NBD
C
FL IKK2WT + ATP*
Time (in mins): 0 2 5 10 30 60
kDa
150
100
75
In vitro Kinase Assay
Autoradiograph
Autophos-phorylation
D
FL IKK2WT + NEMO + ATP*
Time (in mins): 0 2 5 10 30
Autophos-phorylation
NEMO
Coomassie
FL IKK2WT + FL IκBα + ATP*
NEMO
Time (in mins): 0 5 30 0 5 30
FL IκBα
E
FL IKK2WT + ATP*, 30mins
FL IκBα
Inhibitor VII (μM): 0 10 100 0 10 100
FL IκBα
F
ATP*, 30mins
IKK2EE: FL Δ700 Δ664 Trypsinized Δ664
GSTIκBα (1-54): SS AA SS AA SS AA SS AA
GSTIκBα (1-54)

Figure 2

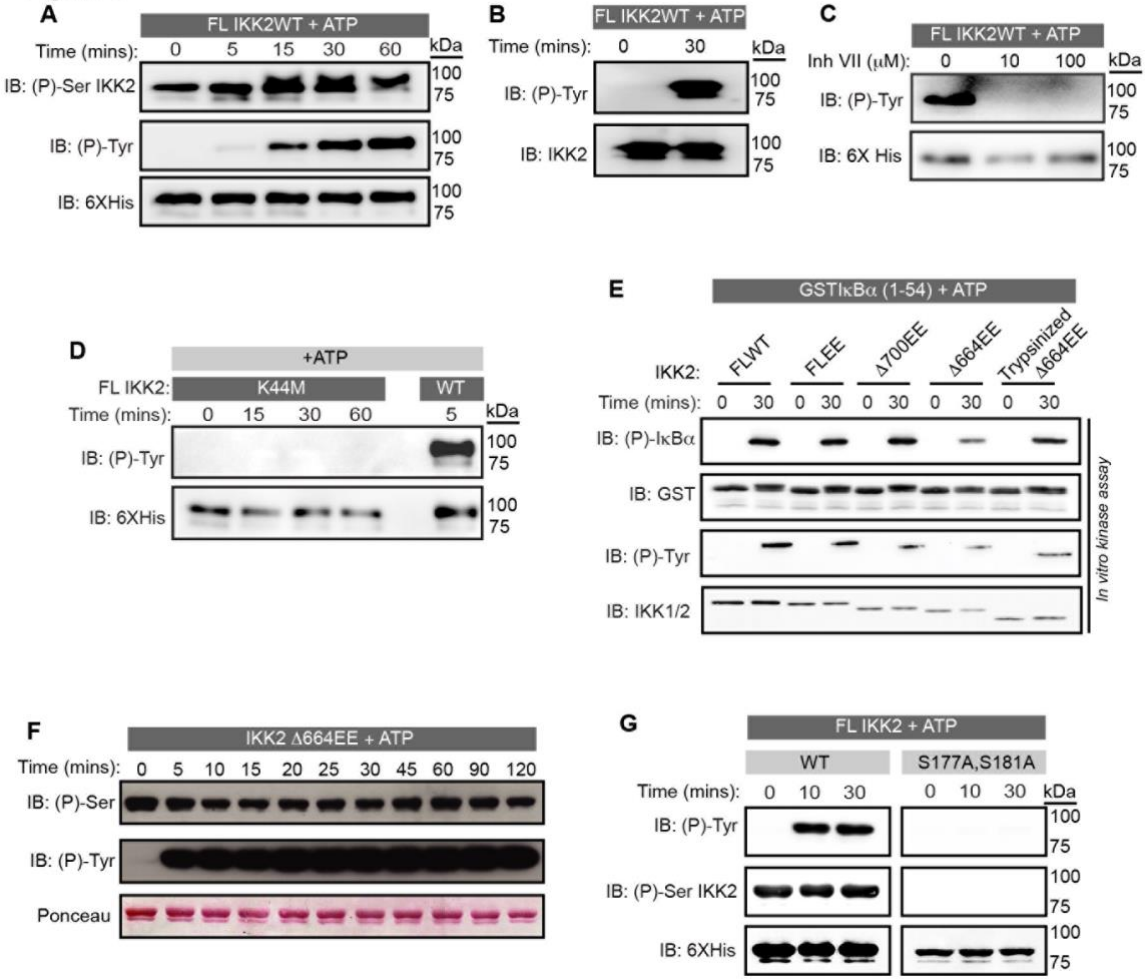
A
FL IKK2WT + ATP
Time (mins): 0 5 15 30 60 kDa
IB: (P)-Ser IKK2
IB: (P)-Tyr
IB: 6XHis
100
75
B
FL IKK2WT + ATP
Time (mins): 0 30 kDa
IB: (P)-Tyr
IB: IKK2
C
FL IKK2WT + ATP
Inh VII (μM): 0 10 100 kDa
IB: (P)-Tyr
IB: 6X His
D
+ATP
FL IKK2: K44M WT
Time (mins): 0 15 30 60 5 kDa
IB: (P)-Tyr
IB: 6XHis
E
GSTIκBα (1-54) + ATP
IKK2: FLWT FLEE Δ700EE Δ664EE Trypsinized Δ664EE
Time (mins): 0 30 0 30 0 30 0 30 0 30
IB: (P)-IκBα
IB: GST
IB: (P)-Tyr
IB: IKK1/2
In vitro kinase assay
F
IKK2 Δ664EE + ATP
Time (mins): 0 5 10 15 20 25 30 45 60 90 120
IB: (P)-Ser
IB: (P)-Tyr
Ponceau
G
FL IKK2 + ATP
WT S177A,S181A
Time (mins): 0 10 30 0 10 30 kDa
IB: (P)-Tyr
IB: (P)-Ser IKK2
IB: 6XHis

Figure 3

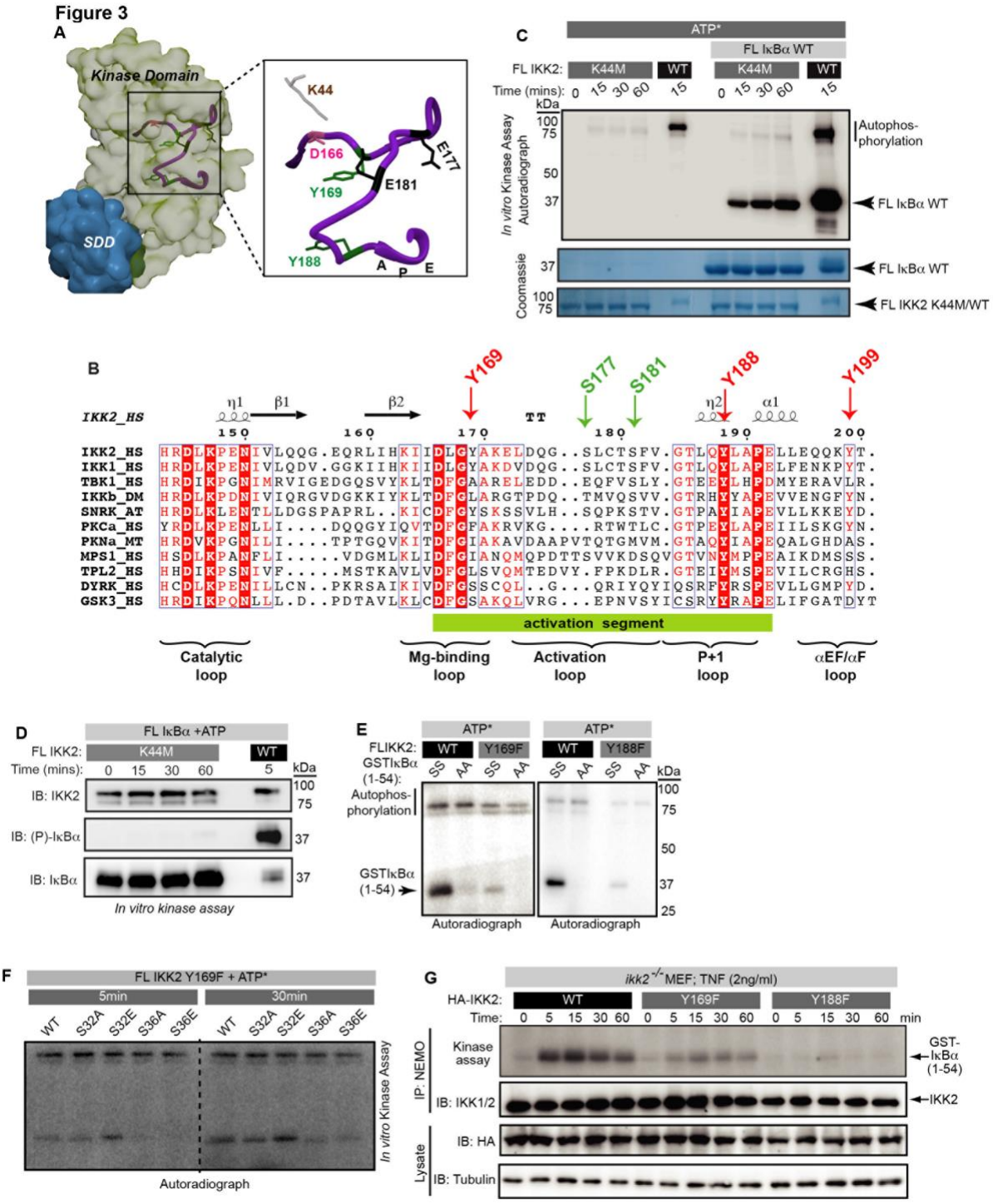
A
Kinase Domain
SDD
K44
D166
Y169
E181
E177
Y188
A
P
E
C
ATP*
FL IKBα WT
FL IKK2:
K44M
WT
K44M
WT
Time (mins): 0 15 30 60 15 0 15 30 60 15
kDa
100
75
50
37
In vitro Kinase Assay Autoradiograph
Autophos-phorylation
FL IKBα WT
Coomassie
37
FL IKBα WT
100
75
FL IKK2 K44M/WT
B
Y169
S177
S181
Y188
Y199
IKK2_HS
η1
β1
β2
TT
η2
α1
150
160
170
180
190
200
IKK2_HS HRDLKPENIVLQQG.EQRLIHKIIDLGYAKELDQG..SLCTSFV.GTLQYLAPELLEQQKYT.
IKK1_HS HRDLKPENIVLQDV.GGKIIHKIIDLGYAKDVDQG..SLCTSFV.GTLQYLAPELFENKPYT.
TBK1_HS HRDIKPGNIMRVIGEDGQSVYKLTDFGAARELEDD..EQFVSLY.GTEEYLHPDMYERAVLR.
IKKb_DM HRDLKPDNIVIQRGVDGKKIYKLTDFGLARGTPDQ..TMVQSVV.GTRHYYAPEVVENGFYN.
SNRK_AT HRDLKLENTLLDGSPAPRL..KICDFGYSKSSVLH..SQPKSTV.GTPAYIAPEVLLKKEYD.
PKCa_HS YRDLKPENLLI....DQQGYIQVTDFGFAKRVKG....RTWTLC.GTPEYLAPEIILSKGYN.
PKNa_MT HRDVKPGNILI....TPTGQVKITDFGIAKAVDAAPVTQTGMVM.GTAQYIAPEQALGHDAS.
MPS1_HS HSDLKPANFLI.....VDGMLKLIDFGIANQMQPDTTSVVKDSQVGTVNYMPPEAIKDMSSS.
TPL2_HS HHDIKPSNIVF.....MSTKAVLVDFGLSVQMTEDVY.FPKDLR.GTEIYMSPEVILCRGHS.
DYRK_HS HCDLKPENILLCN..PKRSAIKIVDFGSSCQL..G...QRIYQYIQSRFYRSPEVLLGMPYD.
GSK3_HS HRDIKPQNLLL.D..PDTAVLKLCDFGSAKQLVRG...EPNVSYICSRYYRAPELIFGATDYT
activation segment
Catalytic loop
Mg-binding loop
Activation loop
P+1 loop
αEF/αF loop
D
FL IKBα +ATP
FL IKK2:
K44M
WT
Time (mins): 0 15 30 60 5
kDa
IB: IKK2
100
75
IB: (P)-IKBα
37
IB: IKBα
37
In vitro kinase assay
E
ATP*
ATP*
FLIKK2:
WT
Y169F
WT
Y188F
GSTIKBα (1-54):
SS AA SS AA SS AA SS AA
kDa
Autophos-phorylation
100
75
50
GSTIKBα (1-54)
37
25
Autoradiograph
Autoradiograph
F
FL IKK2 Y169F + ATP*
5min
30min
WT S32A S32E S36A S36E WT S32A S32E S36A S36E
In vitro Kinase Assay
Autoradiograph
G
ikk2 -/- MEF; TNF (2ng/ml)
HA-IKK2:
WT
Y169F
Y188F
Time: 0 5 15 30 60 0 5 15 30 60 0 5 15 30 60 min
IP: NEMO
Kinase assay
GST-IKBα (1-54)
IB: IKK1/2
IKK2
Lysate
IB: HA
IB: Tubulin

Figure 4

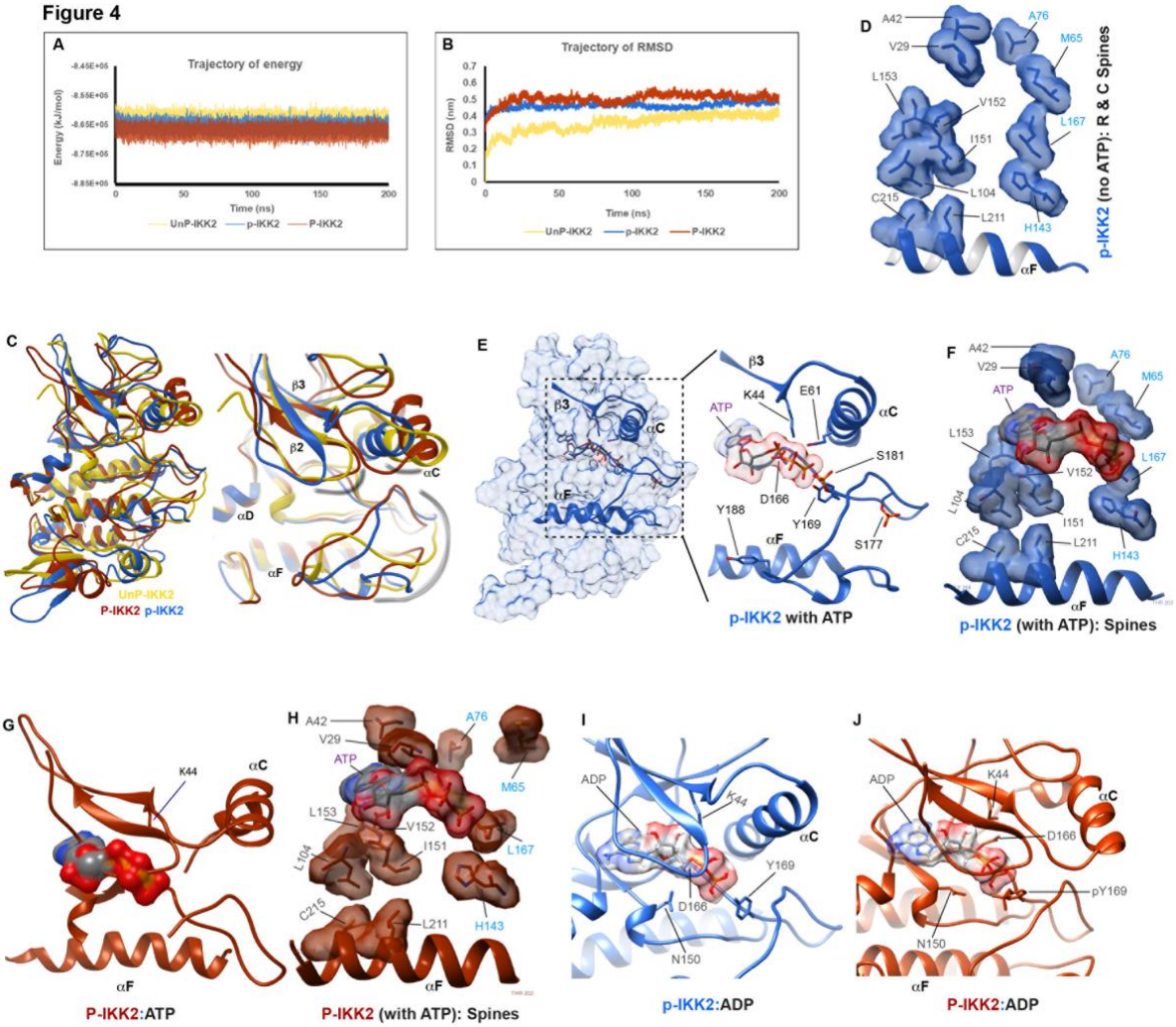
A
Trajectory of energy
Energy (kJ/mol)
Time (ns)
UnP-IKK2
p-IKK2
P-IKK2
B
Trajectory of RMSD
RMSD (nm)
Time (ns)
UnP-IKK2
p-IKK2
P-IKK2
D
A42
V29
L153
V152
I151
L104
C215
L211
αF
A76
M65
L167
H143
p-IKK2 (no ATP): R & C Spines
C
UnP-IKK2
P-IKK2 p-IKK2
β3
β2
αC
αD
αF
E
β3
αC
αF
ATP
K44
E61
S181
D166
Y188
Y169
S177
p-IKK2 with ATP
F
A42
V29
ATP
L153
L104
C215
V152
I151
L211
αF
A76
M65
L167
H143
p-IKK2 (with ATP): Spines
G
K44
αC
αF
P-IKK2:ATP
H
A42
V29
ATP
L153
L104
C215
V152
I151
L211
αF
A76
M65
L167
H143
P-IKK2 (with ATP): Spines
I
ADP
K44
αC
Y169
D166
N150
p-IKK2:ADP
J
ADP
K44
αC
D166
pY169
N150
αF
P-IKK2:ADP

Figure 5

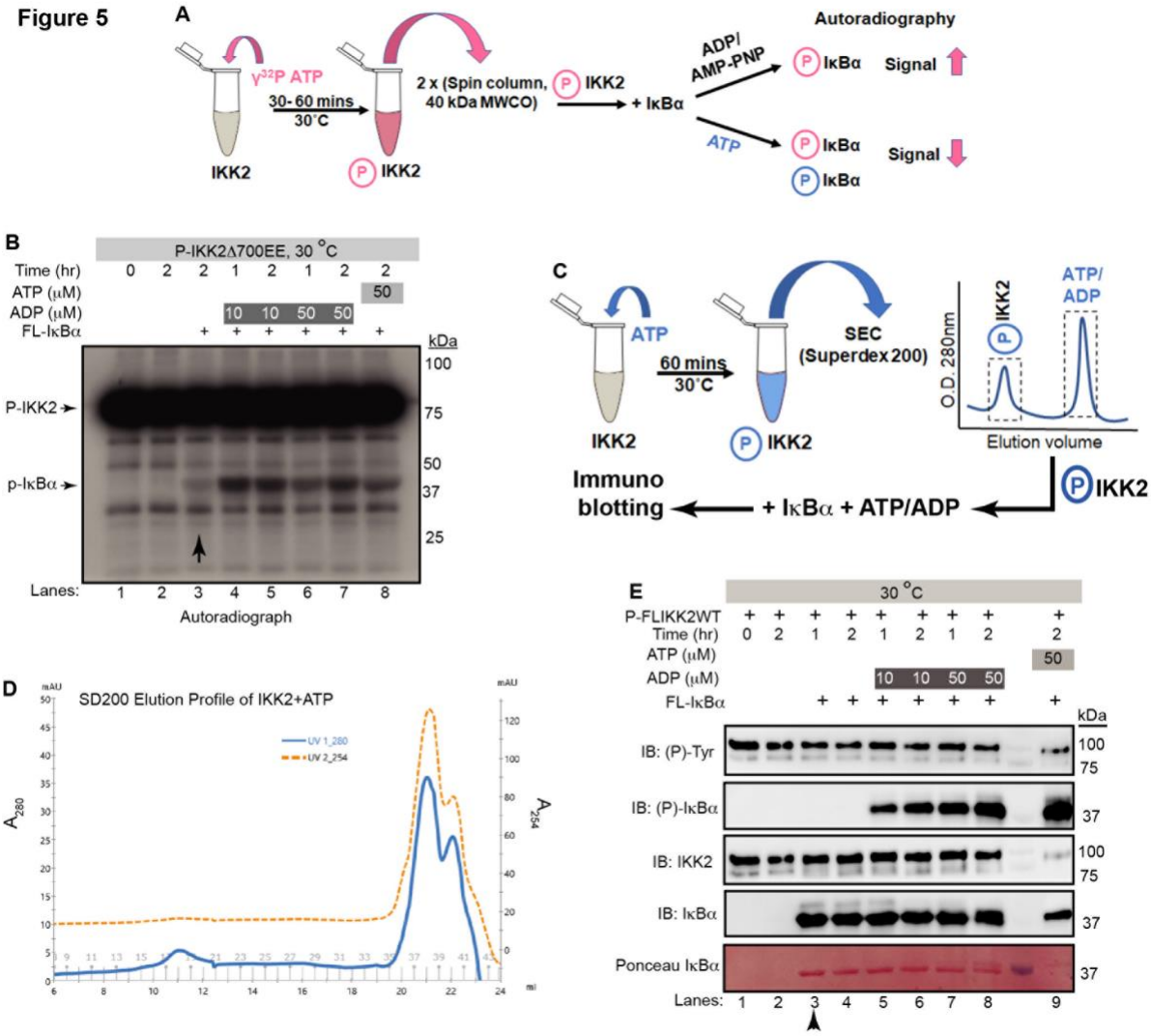

930
931
932

933

Figure 6

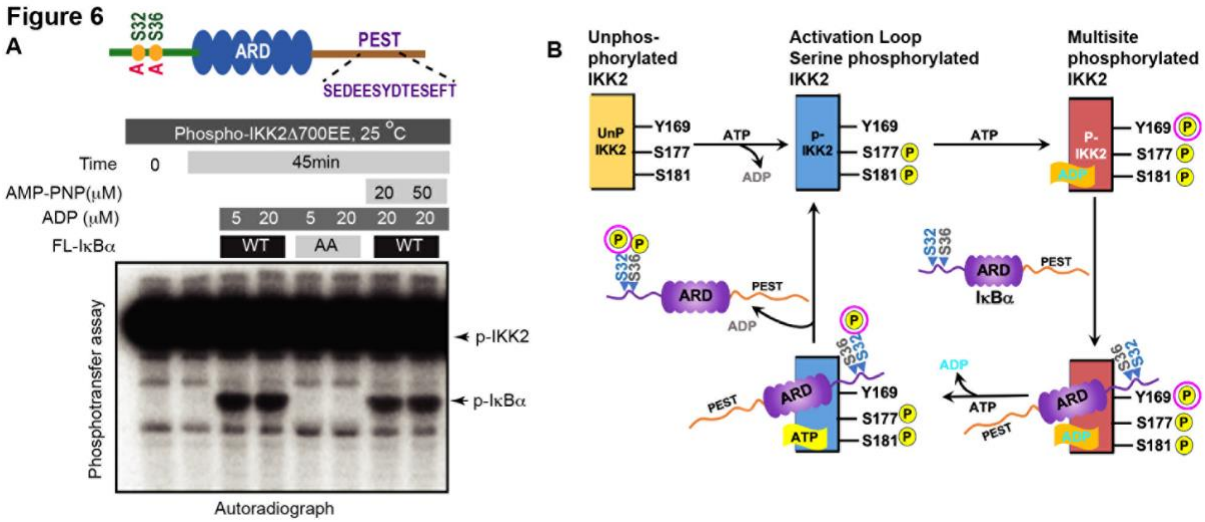

934
935
936
937
938

Figure S1

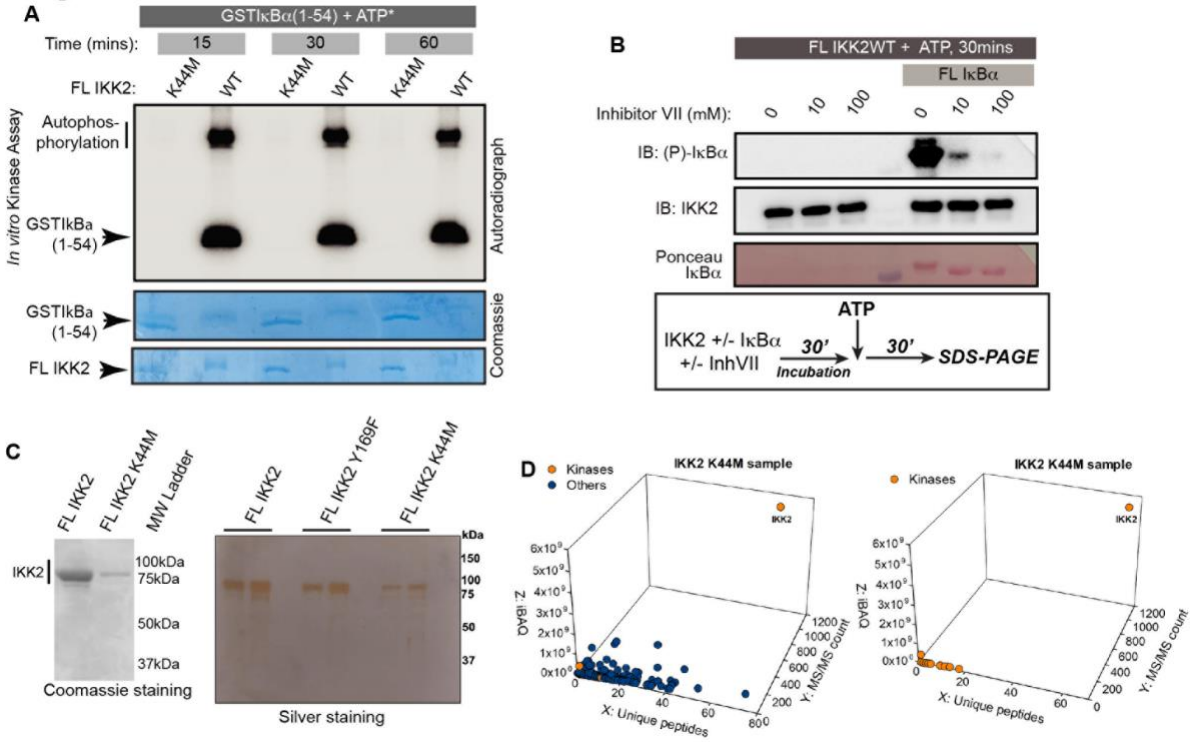
A
GSTIκBα(1-54) + ATP*
Time (mins):
15
30
60
FL IKK2:
K44M
WT
K44M
WT
K44M
WT
In vitro Kinase Assay
Autophos-phorylation
GSTIkBa (1-54)
Autoradiograph
GSTIkBa (1-54)
FL IKK2
Coomassie
B
FL IKK2WT + ATP, 30mins
FL IκBα
Inhibitor VII (mM):
0
10
100
0
10
100
IB: (P)-IκBα
IB: IKK2
Ponceau IκBα
ATP
IKK2 +/- IκBα
+/- InhVII
30'
Incubation
30'
SDS-PAGE
C
FL IKK2
FL IKK2 K44M
MW Ladder
IKK2
100kDa
75kDa
50kDa
37kDa
Coomassie staining
FL IKK2
FL IKK2 Y169F
FL IKK2 K44M
kDa
150
100
75
50
37
Silver staining
D
Kinases
Others
IKK2 K44M sample
IKK2
Z: IBAQ
X: Unique peptides
Y: MS/MS count
Kinases
IKK2 K44M sample
IKK2
Z: IBAQ
X: Unique peptides
Y: MS/MS count

Figure S2

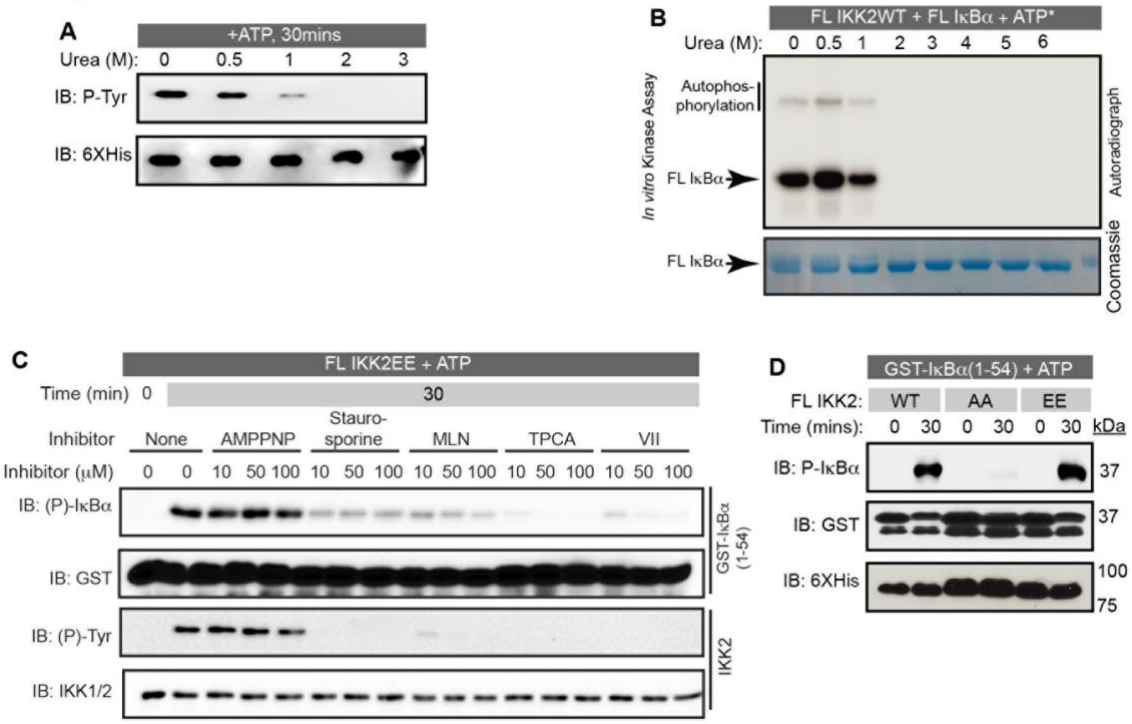
A
+ATP, 30mins
Urea (M): 0 0.5 1 2 3
IB: P-Tyr
IB: 6XHis
B
FL IKK2WT + FL IκBα + ATP*
Urea (M): 0 0.5 1 2 3 4 5 6
In vitro Kinase Assay
Autophos-phorylation
FL IκBα
Autoradiograph
FL IκBα
Coomassie
C
FL IKK2EE + ATP
Time (min) 0 30
Inhibitor None AMPPNP Stauro-sporine MLN TPCA VII
Inhibitor (μM) 0 0 10 50 100 10 50 100 10 50 100 10 50 100 10 50 100
IB: (P)-IκBα
IB: GST
GST-IκBα (1-54)
IB: (P)-Tyr
IB: IKK1/2
IKK2
D
GST-IκBα(1-54) + ATP
FL IKK2: WT AA EE
Time (mins): 0 30 0 30 0 30 kDa
IB: P-IκBα
37
IB: GST
37
IB: 6XHis
100
75

Figure S3

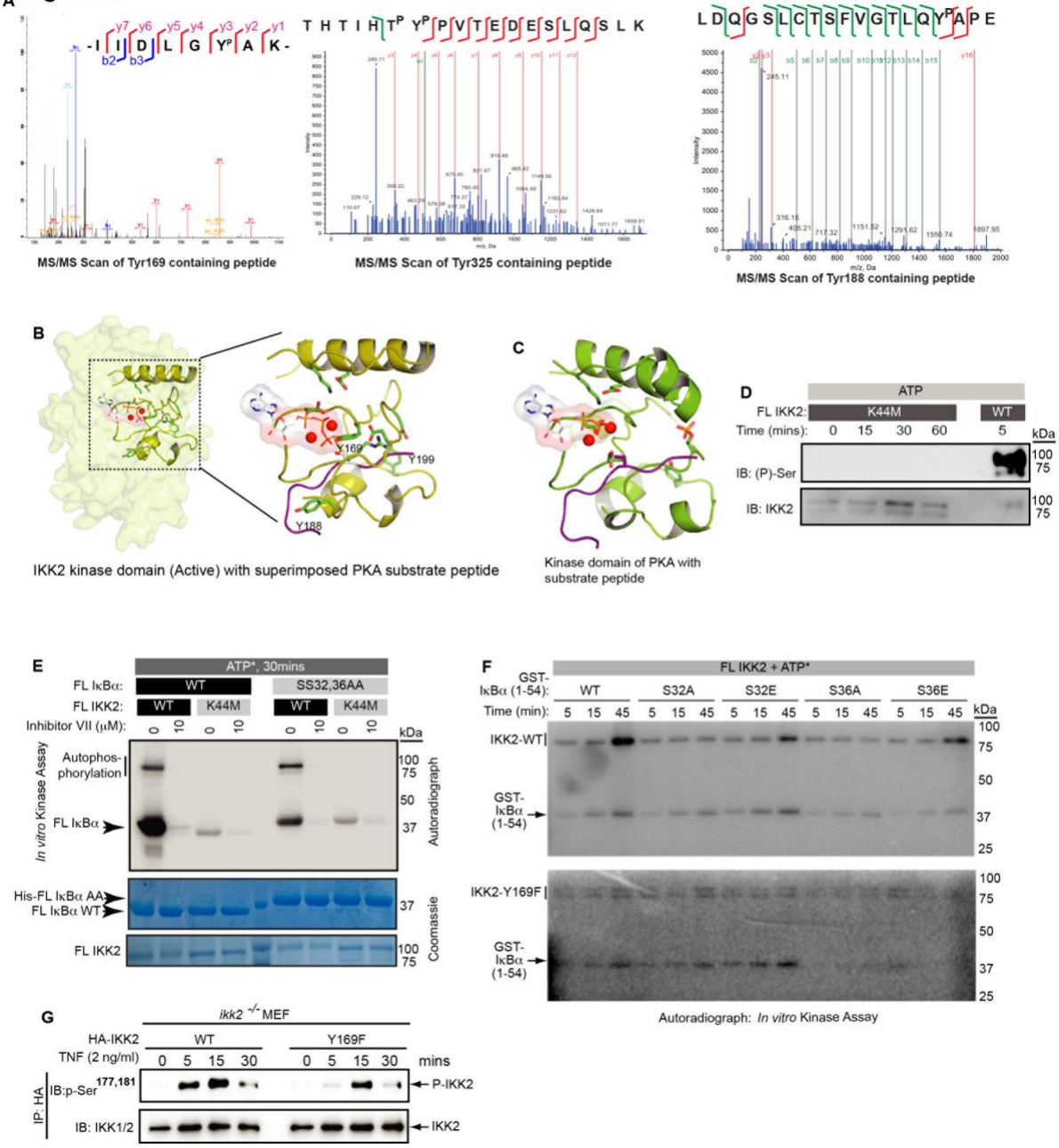
A
MS/MS Scan of Tyr169 containing peptide
MS/MS Scan of Tyr325 containing peptide
MS/MS Scan of Tyr188 containing peptide
B
Y169
Y199
Y188
IKK2 kinase domain (Active) with superimposed PKA substrate peptide
C
Kinase domain of PKA with substrate peptide
D
ATP
FL IKK2:
K44M
WT
Time (mins):
0 15 30 60 5
kDa
IB: (P)-Ser
IB: IKK2
E
ATP*, 30mins
FL IκBα:
WT
SS32,36AA
FL IKK2:
WT
K44M
Inhibitor VII (μM):
In vitro Kinase Assay
Autophos-phorylation
FL IκBα
Autoradiograph
His-FL IκBα AA
FL IκBα WT
FL IKK2
Coomassie
F
FL IKK2 + ATP*
GST-IκBα (1-54):
WT
S32A
S32E
S36A
S36E
Time (min):
5 15 45
IKK2-WT
GST-IκBα (1-54)
IKK2-Y169F
Autoradiograph: In vitro Kinase Assay
G
ikk2 -/- MEF
HA-IKK2
WT
Y169F
TNF (2 ng/ml)
0 5 15 30
mins
IP: HA
IB:p-Ser 177,181
P-IKK2
IB: IKK1/2
IKK2

Figure S4

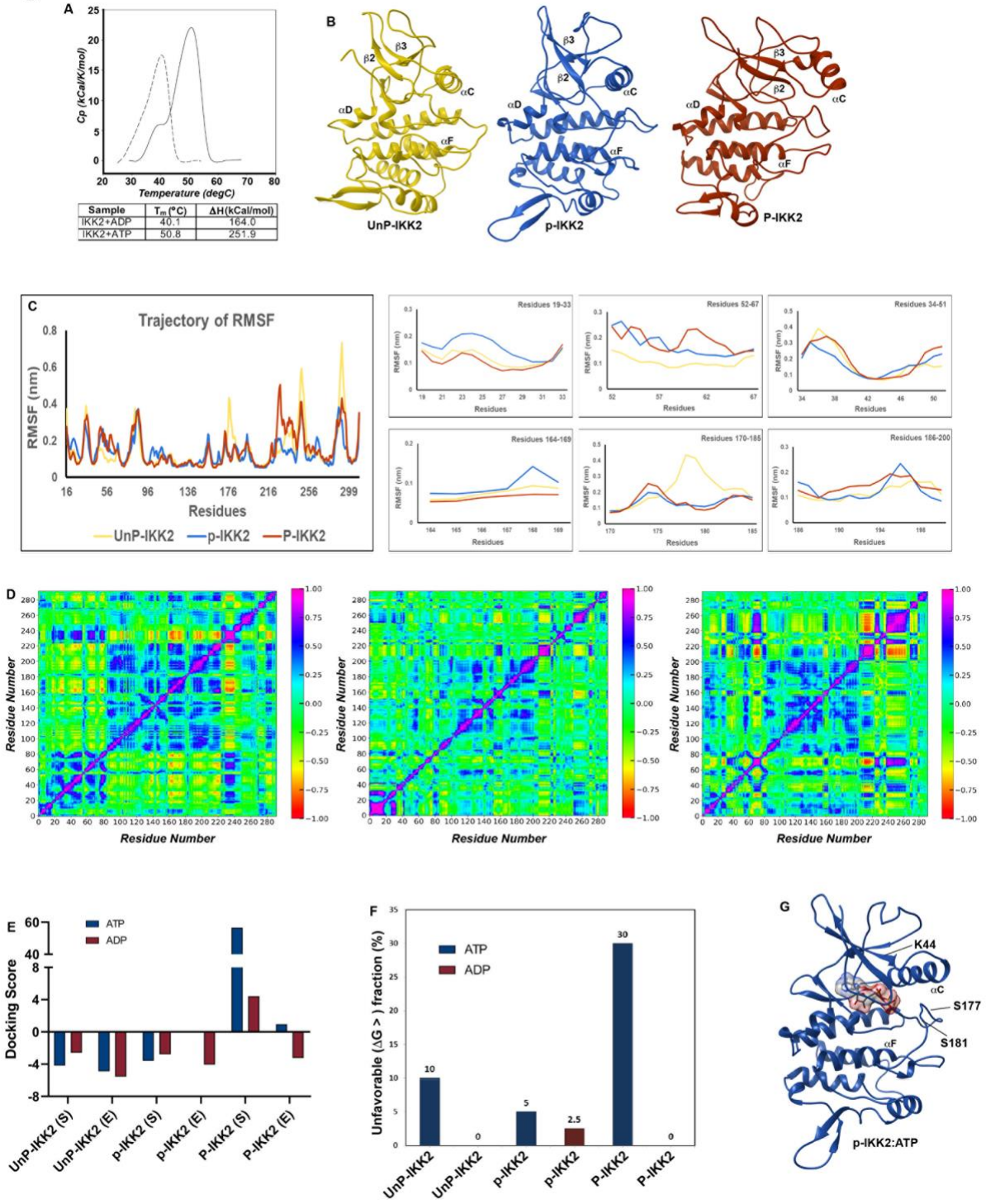

Sample	T_m (°C)	ΔH(kCal/mol)
IKK2+ADP	40.1	164.0
IKK2+ATP	50.8	251.9

Figure S5

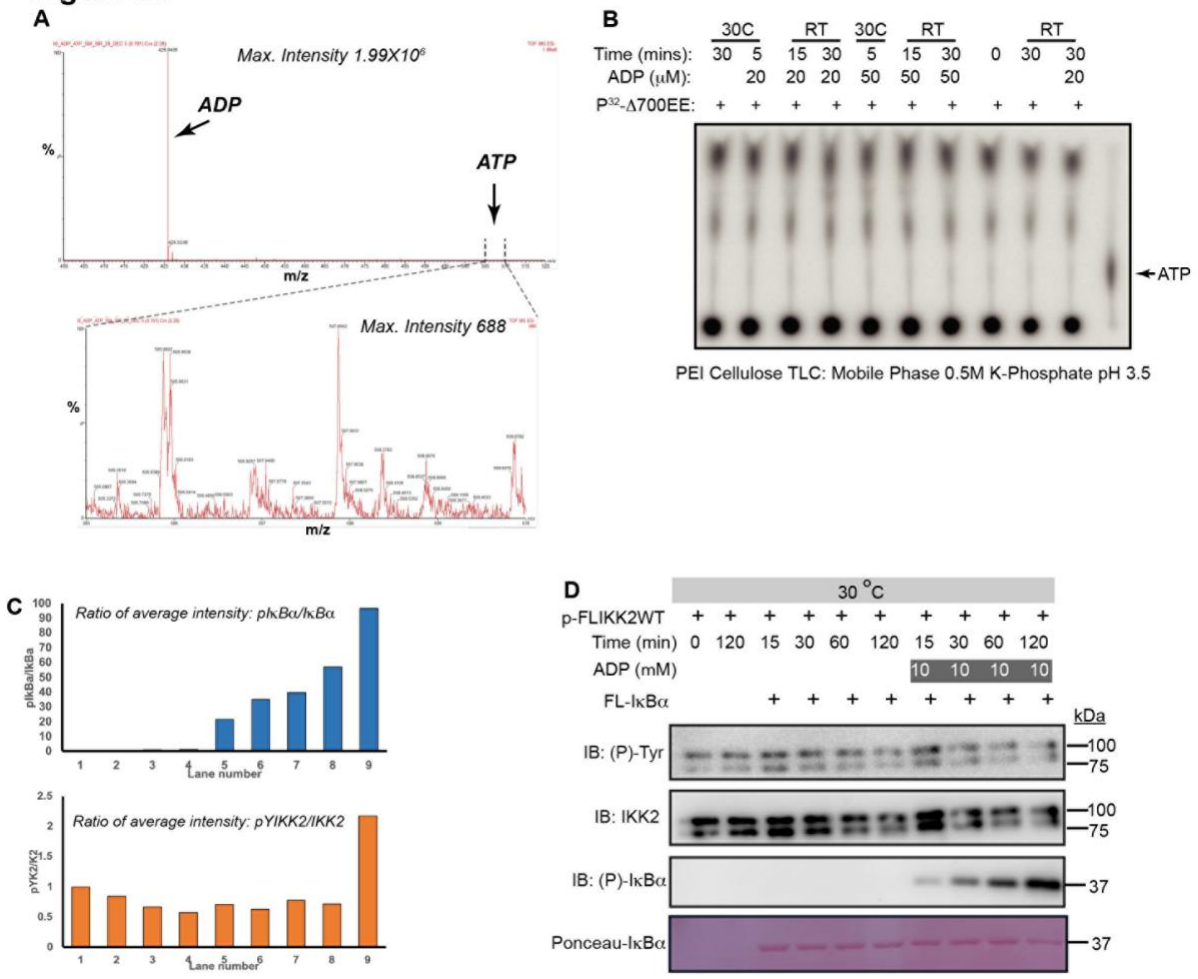
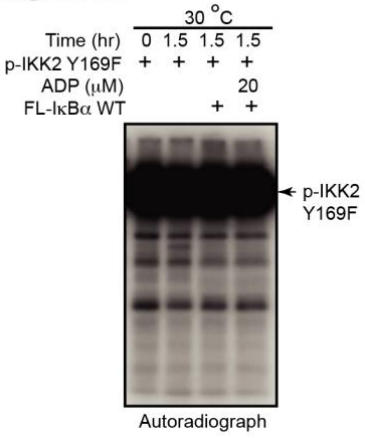
Figure S6